Published for SISSA by Springer

Received: October 4, 2019
Revised: December 2, 2019
Accepted: December 20, 2019
Published: February 25, 2020

Higgs quark flavor violation: simplified models and status of general Two-Higgs-Doublet Model

Juan Herrero-Garcia,[a] **Miguel Nebot,**[c] **Filip Rajec,**[b] **Martin White**[b] **and Anthony G. Williams**[b]

[a] *SISSA/INFN, Via Bonomea 265, Trieste I-34136, Italy*
[b] *ARC Center of Excellence for Particle Physics at Terascale, University of Adelaide, North Terrace, Adelaide, SA 5005, Australia*
[c] *Centro de Física Teórica de Partículas (CFTP), Instituto Superior Técnico (IST), Universidade de Lisboa (UL), Av. Rovisco Pais 1, Lisboa P-1049-001, Portugal*

E-mail: jherrero@sissa.it, miguel.r.nebot.gomez@tecnico.ulisboa.pt, filip.rajec@adelaide.edu.au, martin.white@adelaide.edu.au, anthony.williams@adelaide.edu.au

Abstract: We study quark flavor violating interactions mediated by the Higgs boson h. We consider observables involving a third generation quark, of both the up and the down quark sectors, like $h \to bs$ and $t \to ch$. Using an effective field theory approach we systematically list all the possible tree-level ultraviolet completions, which comprise models with vector-like quarks and/or extra scalars. We provide upper bounds on the flavor violating transitions allowed by current limits stemming from low energy processes, such as meson mixing and $b \to s\gamma$. We find that scenarios with vector-like quarks always have very suppressed flavor-violating transitions, while a general Two-Higgs-Doublet Model may have a sizeable rate. To study the latter case in detail, we perform a full numerical simulation taking into account all relevant theoretical and phenomenological constraints. Our results show that $\mathrm{BR}(t \to ch)$ [$\mathrm{BR}(h \to bs)$] are still allowed at the sub-percent [percent] level, which are being [may be] explored at the LHC [future colliders]. Finally, we have found that the mild mass-splitting discrepancy with respect to the SM in the B_s meson system can be accommodated in the Two-Higgs-Doublet Model. If confirmed, it yields the prediction $\mathrm{BR}(h \to bs) \simeq 10^{-4}$, if the new contribution to the mass-splitting is dominated by tree-level Higgs boson exchange.

Keywords: Phenomenological Models

ArXiv ePrint: 1907.05900

https://doi.org/10.1007/JHEP02(2020)147

JHEP02(2020)147

Contents

JHEP02(2020)147

1 Introduction

In the Standard Model (SM), neutral flavor-changing transitions are absent at tree-level. They arise at the one loop-level with various (additional) sources of suppression like, for example, small elements of the Cabibbo-Kobayashi-Maskawa (CKM) mixing matrix or the Glashow-Iliopoulos-Maiani (GIM) mechanism. It is then clear that they constitute a privileged arena in the search for physics beyond the SM. The discovery in 2012 [1, 2] of a Higgs-like scalar, h in the following, opened the possibility of exploring a new domain in neutral flavor-changing transitions and a strong experimental effort has followed, targeting processes like $t \to ch, uh$ or $h \to \bar{t}^* c\,(u) \to W^- \bar{b} c\,(u)$, and potentially also $h \to bs$, bd. We generically denote these processes as Higgs Quark Flavor Violation (HQFV).

Since $m_t \simeq v/\sqrt{2}$, with v the electroweak symmetry breaking vacuum expectation value of the SM Higgs doublet, the Higgs-top Yukawa coupling is close to 1: if new physics is present, one may expect that such large couplings also manifest in observable transitions of the top quark to up or charm quarks mediated by h. Different studies of top flavor-changing neutral decays can be found in refs. [3–15]. Including those done in the so called 'flavorful models' [13, 14] Current experimental bounds on the branching ratios of those processes are at the 10^{-3} level (see for example refs. [16–19]):

$$\mathrm{BR}(t \to hq) < 7.9 \cdot 10^{-3}, \quad \mathrm{BR}(t \to ch) < 2.2 \cdot 10^{-3}, \qquad \mathrm{BR}(t \to hu) < 2.4 \cdot 10^{-3}, \tag{1.1}$$

at 95% CL. Limits on flavor-changing couplings of the top quark to the Z boson are also quite stringent (see refs. [16, 20–24]):

$$\mathrm{BR}(t \to Zc) < 2.4 \cdot 10^{-4}, \qquad \mathrm{BR}(t \to Zu) < 1.7 \cdot 10^{-4}, \tag{1.2}$$

at 95% CL. Similar constraints apply to $\mathrm{BR}(t \to q\gamma, qg)$ (see for example refs. [25, 26]). Concerning flavor-changing couplings of h to other quarks, the LHC experiments have little direct sensitivity [27], while the ILC could in principle reach subpercent sensitivity for the branching ratios of $h \to bs, bd$ [28]; in ref. [29], it was found that $\mathrm{BR}(h \to bs)$ can be as large as 10^{-1} in Two-Higgs-Doublet Models (2HDMs). Indirect constraints can also be obtained from transitions (i.e. mixing) in the different neutral meson systems, K^0–$\bar{K}^0$ (ds), D^0–$\bar{D}^0$ (cu), B_d^0–$\bar{B}_d^0$ (bd) and B_s^0–$\bar{B}_s^0$ (bs), and from rare decays like $b \to s\gamma$.

The pure effective field theory approach with just the Higgs boson does not cover all the possible phenomenology relevant for HQFV, as was discussed in detail in the case of HLFV in ref. [30]. Therefore, it is crucial to also analyse in detail simplified models, whose extra particles may be subject to more stringent constraints, and to outline the models with the largest possible values of HQFV. We will concentrate on transitions involving the third and second quark generations. The paper is organised as follows. In section 2 we discuss quark flavor violation in the SM and beyond using an EFT approach. We list all possible simplified models and show how the general Two-Higgs-Doublet Model — type III — is the most promising scenario for large HQFV. In section 3, we concentrate on the relevant aspects of the latter. Flavor related constraints are addressed in section 4. A numerical analysis is then presented in section 5. Additional details are covered in the appendices.

JHEP02(2020)147

2 Quark flavor violation in the SM and beyond

In this section we discuss different aspects of quark flavor violation in the SM and beyond. We define the effective Yukawa couplings of the Higgs boson to up and down quarks as

$$\mathcal{L}_{\rm Yuk}^{\rm eff} \equiv -\bar{q}_u \, y_{\rm u} \, q_u \, h - \bar{q}_d \, y_{\rm d} \, q_d \, h \, + \text{H.c.}, \tag{2.1}$$

with summation over omitted generation indices understood: $q_u = (u, c, t)$ and $q_d = (d, s, b)$ are vectors in generation space (the quark fields are in their mass bases) and $y_{\rm u}$ and $y_{\rm d}$ are 3×3 complex Yukawa coupling matrices.

2.1 Effective field theory for Higgs quark flavor violation

In the SM the quark kinetic terms at the renormalizable level read

$$\mathcal{L}_{\rm kin} = \bar{Q}^0 i \not{D} Q^0 + \bar{u}_{\rm R}^0 i \not{D} u_{\rm R}^0 + \bar{d}_{\rm R}^0 i \not{D} d_{\rm R}^0 + \text{H.c.}, \tag{2.2}$$

where, under $\mathrm{SU}(2)_{\rm L}$, $Q^0 = (u_{\rm L}^0, \, d_{\rm L}^0)$ are the quark doublets, and $u_{\rm R}^0$, $(d_{\rm R}^0)$ the up-type (down-type) quark singlets. "0" superscripts correspond to fields in a weak basis while the mass eigenstate basis is unlabelled. D denotes the covariant derivative for the different SM transformations. The SM Yukawa Lagrangian for the up and down-type quarks is

$$\mathcal{L}_{\rm Yuk} = -\bar{Q}^0 \, Y_{\rm u} \, u_{\rm R}^0 \tilde{\Phi} - \bar{Q}^0 \, Y_{\rm d} \, d_{\rm R}^0 \Phi + \text{H.c.}\,, \tag{2.3}$$

where $\Phi = (\Phi^+, \, \Phi_0)^T$ is the SM Higgs doublet. Electroweak symmetry is spontaneously broken by $\langle \Phi \rangle = \frac{v}{\sqrt{2}} \left(\begin{smallmatrix} 0 \\ 1 \end{smallmatrix} \right)$, with $v \simeq 246\,\text{GeV}$, and thus $\mathcal{L}_{\rm Yuk}$ includes mass terms

$$\mathcal{L}_{\rm m_q} = -\bar{u}_{\rm L}^0 \, \frac{v}{\sqrt{2}} Y_{\rm u} \, u_{\rm R}^0 - \bar{d}_{\rm L}^0 \, \frac{v}{\sqrt{2}} Y_{\rm d} \, d_{\rm R}^0 + \text{H.c.}\,. \tag{2.4}$$

The effective Higgs interactions of eq. (2.1), already written in the quark mass basis, have the simple form $-\frac{m_q}{v} \bar{q} q h$ for each quark q, with mass m_q. That is, at tree-level, Higgs couplings to quarks do not violate flavor in the SM. This is an accidental symmetry of the SM, like gauge coupling universality, lepton flavor/number or baryon number, and will be violated at the loop-level or via effective operators. Indeed, at one loop, in the SM $\mathrm{BR}(h \to bs) \sim 10^{-7}$ while $\mathrm{BR}(t \to ch) \sim 10^{-15}$ [31] (the smallness of $t \to ch$ is due to the extra GIM suppression for virtual down quarks). Beyond eq. (2.3), the lowest dimension quark flavor-changing operators involving the Higgs field appear at dimension 6. We refer to them in the following as *Yukawa operators*. Denoting the scale of new physics by Λ, the effective Lagrangians for up and down quarks read respectively

$$\mathcal{L}_{\rm up}^{\rm eff} = \frac{-1}{\Lambda^2} \bar{Q}^0 \, C_{\rm u}^0 \, u_{\rm R}^0 \tilde{\Phi} \, (\Phi^\dagger \Phi) + \text{H.c.}\,, \tag{2.5}$$

and

$$\mathcal{L}_{\rm down}^{\rm eff} = \frac{-1}{\Lambda^2} \bar{Q}^0 \, C_{\rm d}^0 \, d_{\rm R}^0 \Phi \, (\Phi^\dagger \Phi) + \text{H.c.}\,. \tag{2.6}$$

JHEP02(2020)147

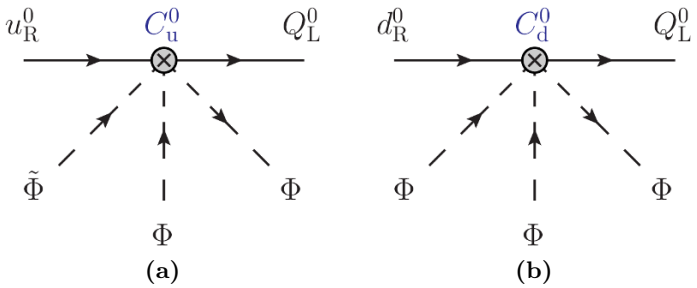

Figure 1. *Yukawa operators* in eqs. (2.5) and (2.6).

They are represented in figure 1. After electroweak symmetry breaking (EWSB), the diagonalization of the complete quark mass matrices is

$$D_{\rm u} = U_L^{u\dagger} \frac{v}{\sqrt{2}} \left(Y_{\rm u} + C^0_{\rm u} \frac{v^2}{2\Lambda^2} \right) U_R^u \,, \tag{2.7}$$

$$D_{\rm d} = U_L^{d\dagger} \frac{v}{\sqrt{2}} \left(Y_{\rm d} + C^0_{\rm d} \frac{v^2}{2\Lambda^2} \right) U_R^d \,. \tag{2.8}$$

Now the effective Yukawas of the Higgs in eq. (2.1) read

$$y_{\rm u} = \frac{D_u}{v} + C_{\rm u} \frac{v^2}{\sqrt{2}\Lambda^2} \,, \qquad y_{\rm d} = \frac{D_d}{v} + C_{\rm d} \frac{v^2}{\sqrt{2}\Lambda^2} \,, \tag{2.9}$$

where $C_{\rm u} = U_L^{u\dagger} C^0_{\rm u} U_R^u$ and $C_{\rm d} = U_L^{d\dagger} C^0_{\rm d} U_R^d$: the Higgs Yukawa interactions are no longer diagonal at tree-level, generating HQFV. Without loss of generality, we can use the mass basis for the up-type quarks. The quark charged current interactions read $\mathcal{L}_W = \frac{g}{\sqrt{2}} \bar{u}_{\rm L} \gamma^\mu V d_{\rm L} W^+_\mu$ + H.c., where the CKM matrix is $V = U_L^d$.

2.2 Simplified models

In this section we discuss tree-level simplified models by "opening" the Yukawa operators for up and down quarks given in eqs. (2.5) and (2.6), respectively. This means that we give the nature and quantum numbers of the possible heavy mediators that could generate the previous operators after being integrated-out. For down quarks the operators are represented in figure 2. Tables 1 (for up quarks) and 2 (for down quarks) list all the possible simplified models. We follow the same approach used for the case of Higgs lepton flavor violation in ref. [30]. We have considered 2 extra particles at most: the new particles considered in each model are given in the second column of tables 1 and 2, where S stands for scalar and F for fermion. The $({\rm SU}(2)_{\rm L}, {\rm Y})$ quantum numbers are given in the third column. In the last column, the form of the contributions to $C_{\rm u,d}$ is provided in terms of the masses of the new particles (m_F or m_{F_j} for fermions, m_S or m_{S_j} for scalars) and of generic new physics couplings: scalar quartic couplings λ, dimensionful trilinear scalar couplings μ, μ_j, and Yukawa-type couplings $f_{\rm q}$, where ${\rm q} = {\rm u}, {\rm d}, {\rm Q}$ refers to the SM field involved (in that order of preference if two SM fields are involved) or ${\rm q} = {\rm VLQ}$ for an interaction term involving two new vector-like quarks. Note that the CKM matrix V enters in the expression of $C_{\rm d}$ (down quarks).

JHEP02(2020)147

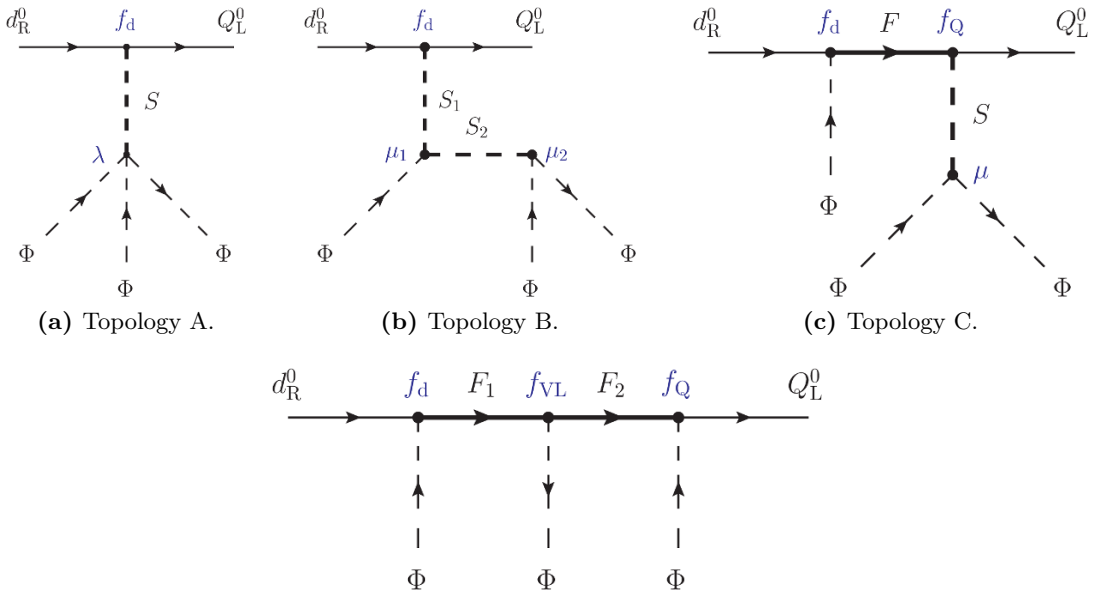

(a) Topology A. **(b)** Topology B. **(c)** Topology C.

(d) Topology D.

Figure 2. Tree-level topologies of the *Yukawa operator* for down-type quarks, see table 2. Similar diagrams exist for up-type quarks.

2.2.1 The Yukawa operators

The tree-level simplified models of the up and down *Yukawa operators* that only involve scalars are identical to the ones discussed for Higgs lepton flavor violation in ref. [30] (see table 3 therein), denoted by topologies A and B. Topology A corresponds to the 2HDM, which has been extensively studied in all its variants (see for example refs. [29, 32–39]). In sections 3 to 4 different aspects of the general 2HDM are discussed, and a full numerical analysis of HQFV is presented in section 5. Topology B adds new scalars to topology A, while the flavor structure is still dominated by the couplings of the scalar doublet to the quark bilinears. Topologies C^i $(i = 1, \ldots, 4)$ and D^j $(j = 1, \ldots, 3)$ correspond to models where vector-like quarks (VLQ) are also present (VLQ are, of course, color triplets). Models like these have been studied in the literature, see for instance refs. [40–52].

2.2.2 The derivative operators

Besides the *Yukawa operators*, there are other dimension 6 operators which generate HQFV. They involve covariant derivatives, and therefore we denote them as *Derivative operators*. These are plotted in figure 3 and are listed in table 3. They are related by the equations of motion (EOM) to the *Yukawa operators* previously considered. This implies that, for instance, for up-type quarks their contribution to HQFV will be proportional to the quark masses. It is illustrative to consider them specifically. This is because some simple UV models directly generate them, and as we will show they are very constrained by limits from flavor-changing processes involving the Z boson. Moreover, some of the particles that generated the previous *Yukawa operators* also generate these ones.

JHEP02(2020)147

Topology	Particles	Representations	$C_{\rm u}/\Lambda^2$
$A_{\rm u}$	S	$(2,1/2)_S$	$\frac{f_{\rm u}\lambda}{m_S^2}$
$B_{\rm u}$	$S_1 \oplus S_2$	$(2,1/2)_S \oplus (1,0)_S, (3,0)_S, (3,-1)_S$	$\frac{f_{\rm u}\mu_1\mu_2}{m_{S_1}^2 m_{S_2}^2}$
$C_{\rm u}^1$	$S \oplus F$	$(2,1/6)_F \oplus (1,0)_S, (3,0)_S$	
$C_{\rm u}^2$	$S \oplus F$	$(2,7/6)_F \oplus (3,-1)_S$	
$C_{\rm u}^3$	$S \oplus F$	$(1,2/3)_F \oplus (1,0)_S,\ (3,2/3)_F \oplus\ (3,0)_S$	$\frac{f_{\rm Q} f_{\rm u}\mu}{m_F m_S^2}$
$C_{\rm u}^4$	$S \oplus F$	$(3,-1/3)_F \oplus (3,-1)_S$	
$D_{\rm u}^1$	$F_1 \oplus F_2$	$(2,7/6)_F \oplus (1,2/3)_F, (3,2/3)_F$	
$D_{\rm u}^2$	$F_1 \oplus F_2$	$(2,1/6)_F \oplus (1,2/3)_F, (3,2/3)_F$	$\frac{f_{\rm Q} f_{\rm VLQ} f_{\rm u}}{m_{F_1} m_{F_2}}$
$D_{\rm u}^3$	$F_1 \oplus F_2$	$(2,1/6)_F \oplus (1,-1/3)_F, (3,-1/3)_F$	

Table 1. Tree-level topologies of the *Yukawa operator* for up-type quarks, see eq. (2.5). S stands for scalar, F for fermion, with the representation under $(\mathrm{SU}(2)_{\rm L}, \mathrm{Y})$. All vector-like fermions are color triplets, while the scalars are color singlets.

Topology	Particles	Representations	$C_{\rm d}/\Lambda^2$
$A_{\rm d}$	S	$(2,-1/2)_S$	$V^\dagger \frac{f_{\rm d}\lambda}{m_S^2}$
$B_{\rm d}$	$S_1 \oplus S_2$	$(2,-1/2)_S \oplus (1,0)_S, (3,0)_S, (3,1)_S$	$V^\dagger \frac{f_{\rm d}\mu_1\mu_2}{m_{S_1}^2 m_{S_2}^2}$
$C_{\rm d}^1$	$S \oplus F$	$(2,1/6)_F \oplus (1,0)_S, (3,0)_S$	
$C_{\rm d}^2$	$S \oplus F$	$(2,-5/6)_F \oplus (3,1)_S$	
$C_{\rm d}^3$	$S \oplus F$	$(1,-1/3)_F \oplus (1,0)_S,\ (3,-1/3)_F \oplus\ (3,0)_S$	$V^\dagger \frac{f_{\rm Q} f_{\rm d}\mu}{m_F m_S^2}$
$C_{\rm d}^4$	$S \oplus F$	$(3,2/3)_F \oplus (3,1)_S$	
$D_{\rm d}^1$	$F_1 \oplus F_2$	$(2,1/6)_F \oplus (1,2/3)_F, (3,2/3)_F$	
$D_{\rm d}^2$	$F_1 \oplus F_2$	$(2,1/6)_F \oplus (1,-1/3)_F, (3,-1/3)_F$	$V^\dagger \frac{f_{\rm Q} f_{\rm VLQ} f_{\rm d}}{m_{F_1} m_{F_2}}$
$D_{\rm d}^3$	$F_1 \oplus F_2$	$(2,-5/6)_F \oplus (1,-1/3)_F, (3,-1/3)_F$	

Table 2. Similar to table 1 for the *Yukawa operator* of down-type quarks, see eq. (2.6).

JHEP02(2020)147

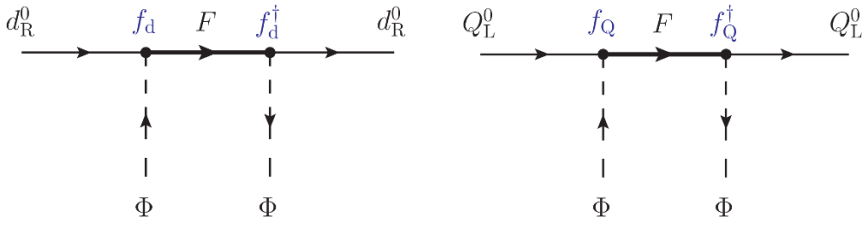

(a) Topology E^1_d. **(b)** Topology $E^{3,4}_u$.

Figure 3. Examples of tree-level topologies (E) of the *Derivative operators*, see table 3.

Operator	Topology	Particles	$Zu_\alpha u_\beta$	$Zd_\alpha d_\beta$	$Wd_\alpha u_\beta$	$hq_\alpha q_\beta$
$(\bar{u}_{\rm R}\Phi^\dagger)i\not{D}(u_{\rm R}\,\Phi)$	$E^1_{\rm u}$	$(2,7/6)_F$	-1			$\frac{\lvert f_{\rm u}\rvert^2 m_{\rm u} v}{m_F^2}$
$(\bar{u}_{\rm R}\Phi^T)i\not{D}(u_{\rm R}\,\Phi^*)$	$E^2_{\rm u}$	$(2,1/6)_F$	$+1$			$\frac{\lvert f_{\rm u}\rvert^2 m_{\rm u} v}{m_F^2}$
$(\bar{Q}\tilde{\Phi})i\not{D}(\tilde{\Phi}^\dagger Q)$	$E^3_{\rm u}$	$(1,2/3)_F$	-1		-1	$\frac{\lvert f_{\rm Q}\rvert^2 m_{\rm u} v}{m_F^2}$
$(\bar{Q}\vec{\tau}\tilde{\Phi})i\not{D}(\tilde{\Phi}^\dagger\vec{\tau}Q)$	$E^4_{\rm u}$	$(3,2/3)_F$	-1	-2	$+1$	$\frac{\lvert f_{\rm Q}\rvert^2 m_{\rm u} v}{m_F^2}$
$(\bar{d}_{\rm R}\Phi^\dagger)i\not{D}(d_{\rm R}\,\Phi)$	$E^1_{\rm d}$	$(2,1/6)_F$		-1		$\frac{\lvert f_{\rm d}\rvert^2 m_{\rm d} v}{m_F^2}$
$(\bar{d}_{\rm R}\Phi^T)i\not{D}(d_{\rm R}\,\Phi^*)$	$E^2_{\rm d}$	$(2,-5/6)_F$		$+1$		$\frac{\lvert f_{\rm d}\rvert^2 m_{\rm d} v}{m_F^2}$
$(\bar{Q}\Phi)i\not{D}(\Phi^\dagger\,Q)$	$E^3_{\rm d}$	$(1,-1/3)_F$		$+1$	-1	$\frac{\lvert V^\dagger f_{\rm Q}\rvert^2 m_{\rm d} v}{m_F^2}$
$(\bar{Q}\vec{\tau}\Phi)i\not{D}(\Phi^\dagger\,\vec{\tau}Q)$	$E^4_{\rm d}$	$(3,-1/3)_F$	$+2$	$+1$	$+1$	$\frac{\lvert V^\dagger f_{\rm Q}\rvert^2 m_{\rm d} v}{m_F^2}$

Table 3. Tree-level topologies of the *Derivative operators*. The Higgs interactions in the last column correspond to the effective Yukawa couplings y_q, provided in eq. (2.1), with $q = u$ ($q = d$) for the first (last) four rows. Z couplings are in units of $y_q v/m_q \times e/(2c_W s_W)$, while W ones are in units of $V\, y_q v/m_q \times e/(2\sqrt{2}s_W)$.

We show further details regarding the generation of flavor-changing neutral currents from these operators in appendix A. The key point is that the flavor-changing neutral currents appear because of a mismatch between the quantum numbers on which the covariant derivative acts for the case of the *Derivative operators* and for the renormalizable kinetic terms of eq. (2.2) [30]. In table 3 we also list all the possible simplified models of the *Derivative operators* (third column), as well as the new Z-mediated quark flavor violating, charged-current (CC) and HQFV interactions. The Higgs interactions in the last column are given in terms of the effective Yukawa couplings y_q provided in eq. (2.1). Notice that Z and W-boson interactions are independent of the quark mass involved. The chirality of the quarks involved can be understood from the operators.

We have seen using the *Derivative operators* that in the models with VLQ, both ZQFV and HQFV are related. We can derive the relationship among both explicitly, see also

JHEP02(2020)147

refs. [30, 42, 44]. In models with VLQ, charged current couplings read

$$\mathcal{L}_W = \frac{g}{\sqrt{2}}\left(\bar{u}_{\rm L}\gamma^\mu V_L d_{\rm L} + \bar{u}_{\rm R}\gamma^\mu V_R d_{\rm R}\right) W^+_\mu + \text{H.c.}, \tag{2.10}$$

with V_L the "enlarged" CKM matrix, and V_R its right-handed counterpart (which arises when VLQ which are not $\mathrm{SU}(2)_L$ singlets are considered). V_L is now a $n_u \times n_d$ matrix for n_u up quarks and n_d down quarks, and it is not unitary.[1] The neutral current couplings read

$$\mathcal{L}_Z = \frac{g}{2c_W}\left(\bar{d}_{\rm L}\gamma^\mu X^d_{\rm L} d_{\rm L} + \bar{d}_{\rm R}\gamma^\mu X^d_{\rm R} d_{\rm R} - \bar{u}_{\rm L}\gamma^\mu X^u_{\rm L} u_{\rm L} - \bar{u}_{\rm R}\gamma^\mu X^u_{\rm R} u_{\rm R} - 2s^2_W J^\mu_{\rm em}\right) Z_\mu, \tag{2.11}$$

where

$$X^u_{\rm L} = V_L V_L^\dagger, \quad X^u_{\rm R} = V_R V_R^\dagger, \quad X^d_{\rm L} = V_L^\dagger V_L, \quad X^d_{\rm R} = V_R^\dagger V_R. \tag{2.12}$$

The Z flavor-changing interactions in $\mathcal{L}_Z$ are given by the non-unitarity of the mixing matrices. Similarly, the Yukawa couplings to h read

$$\begin{aligned}\mathcal{L}_h = &-\frac{h}{v}\bar{u}_{\rm L}\left(X^u_{\rm L} D_u + D_u X^u_{\rm R} - 2X^u_{\rm L} D_u X^u_{\rm R}\right) u_{\rm R} \\ &- \frac{h}{v}\bar{d}_{\rm L}\left(X^d_{\rm L} D_d + D_d X^d_{\rm R} - 2X^d_{\rm L} D_d X^d_{\rm R}\right) d_{\rm R} + \text{H.c.}\,.\end{aligned} \tag{2.13}$$

Consider for example the $h\bar{t}_L c_R$ coupling; in the notation of eq. (2.1)

$$v(y_{\rm u})_{tc} = (X^u_{\rm L})_{tc} m_c + m_t (X^u_{\rm R})_{tc} - 2(X^u_{\rm L} D_u X^u_{\rm R})_{tc}\,. \tag{2.14}$$

The first term corresponds to the *Derivative operator* $E^{3\,(4)}_{\rm u}$, where a VLQ singlet (triplet) is exchanged, while the second term corresponds to $E^{1,2}_{\rm u}$, where a VLQ doublet is exchanged. These contributions pick up a quark mass, as would be the case if one uses EOM to transform the operators. The last contribution corresponds to topology D of the up-quark *Yukawa operator*, where two types of VLQ are exchanged (a doublet plus a singlet or triplet). Therefore we can estimate the contribution as

$$v(y_{\rm u})_{tc} \approx \left|\frac{f_Q v}{m_{F_{1,3}}}\right|^2_{tc} m_c + \left|\frac{f_u v}{m_{F_2}}\right|^2_{tc} m_t - 2\left(\frac{f_Q v}{m_{F_{1,3}}} f_{\rm VLQ} v \frac{f_u v}{m_{F_2}}\right)_{tc}. \tag{2.15}$$

In this example, the dominant term for top HQFV is the second or the last one. For bottom HQFV clearly the last term dominates unless $f_{\rm VLQ} v < m_b$. Correspondingly, the deviations from 3×3 unitarity of the CKM mixing matrix due to the presence of VLQ are

$$V_L^\dagger V_L \approx \mathbf{1} - \frac{|f_{\rm Q}|^2}{m^2_F}\frac{e\,v^2}{\sqrt{2}s_W}, \tag{2.16}$$

where now $f_{\rm Q}$ and m_F are matrices in flavor space.

[1] It can be embedded, however, in a larger $n_L \times n_L$ unitary matrix, with n_L the number of left-handed quark fields; for example, for a model with only an up-type singlet VLQ, V_L is a 4×3 submatrix of a 4×4 unitary matrix.

JHEP02(2020)147

2.3 Estimates for models with vector-like quarks

The phenomenology of VLQ models has been scrutinised in the literature [8, 40–52]. For example, ref. [51] addresses in some detail constraints arising from meson mixing.

For models with just VLQ, since ZQFV and deviations from 3×3 unitarity of CC interactions are related to HQFV, one can estimate some simple upper bounds on $h \to bs$ and $t \to ch$. In the up sector, from eq. (2.11), the leading contribution to $t \to Zc$ (which occurs at tree-level), ignoring QCD corrections, is

$$\Gamma(t \to Zc) = \frac{m_t^3}{32\pi v^2} \left(|(X^u_{\rm L})_{ct}|^2 + |(X^u_{\rm R})_{ct}|^2 \right) \mathcal{F}(m_Z, m_t) \,, \tag{2.17}$$

where $\mathcal{F}(m_X, m_t) = (1 - m_X^2/m_t^2)^2(1 + 2m_X^2/m_t^2)$. Since the top total decay width $\Gamma_t = \Gamma(t \to Wb)$ remains essentially unchanged, using $\mathcal{F}(m_W, m_t) \approx \mathcal{F}(m_Z, m_t)$, the experimental bound on $\mathrm{BR}(t \to Zc)$ in eq. (1.2) gives

$$\left(|(X^u_{\rm L})_{ct}|^2 + |(X^u_{\rm R})_{ct}|^2 \right) < \mathrm{BR}(t \to Zc)_{\rm exp} \,. \tag{2.18}$$

Concerning $t \to ch$ decays, with $m_c \ll m_h, m_t$, from the first line of eq. (2.13) we have

$$-\frac{h}{v} \bar{c}_{\rm L} \left[(X^u_{\rm L})_{ct} m_t - 2 (X^u_{\rm L})_{cq} m_q (X^u_{\rm R})_{qt} \right] t_{\rm R} . \tag{2.19}$$

If the mixing with heavy VLQ is suppressed compared to the top exchange, the dominant contribution in the second term is $q = t$ and $(X^u_{\rm R})_{tt} \simeq 1$, and thus we are left with an interaction term $-\frac{m_t}{v} h (X^u_{\rm L})_{ct} \bar{c}_{\rm L} t_{\rm R}$. From the hermitian conjugate term in (2.13), the interaction term with flipped chiralities is $-\frac{m_t}{v} h (X^u_{\rm R})_{ct} \bar{c}_{\rm R} t_{\rm L}$. Then, the leading prediction for $t \to ch$ (again, tree-level, $m_c \to 0$ and no QCD corrections) is

$$\Gamma(t \to ch) = \frac{m_t^3}{32\pi v^2} \left(|(X^u_{\rm L})_{ct}|^2 + |(X^u_{\rm R})_{ct}|^2 \right) \mathcal{H}(m_h, m_t) \,, \tag{2.20}$$

where $\mathcal{H}(m_h, m_t) = (1 - m_h^2/m_t^2)^2$. Combining eqs. (2.17) and (2.20), the experimental bound on $\mathrm{BR}(t \to Zc)$ translates into a bound

$$\mathrm{BR}(t \to ch) < \mathrm{BR}(t \to Zc)_{\rm exp} \frac{\mathcal{H}(m_h, m_t)}{\mathcal{F}(m_Z, m_t)} \simeq 7 \times 10^{-5} \,, \tag{2.21}$$

which is two orders of magnitude smaller than the current sensitivity, eq. (1.1).

For $b \to s$ transitions, although a similar reasoning would lead to straightforward bounds on the allowed values of $\mathrm{BR}(h \to bs)$ in the context of VLQ extensions of the SM, experimental input on $b - s$ transitions from $Z \to bs$ is much poorer than low energy constraints from B_s mixing, $B_s \to \mu^+\mu^-$ or $b \to s\gamma$ transitions. For the latter, diagrams with chirality flips in the VLQ lines dominate the processes, in an analogous way to those discussed in ref. [30] for the lepton sector, further suppressing HQFV. Typical bounds on Z_{bs} couplings from detailed studies in the literature are below the 10^{-4} level; one can thus estimate a rough upper bound on $\mathrm{BR}(h \to bs)$ in the context of VLQ extensions

$$\mathrm{BR}(h \to bs) < |Z_{bs}|^2 \frac{3}{8\pi} \frac{m_h}{\Gamma_h} \simeq 10^{-5} \,. \tag{2.22}$$

JHEP02(2020)147

Equations (2.21) and (2.22) illustrate that HQFV in extensions with just VLQ, with branching ratios forced to be below the 10^{-5} level by ZQFV, are much less promising than scenarios with HQFV arising from a richer scalar sector. Moreover, the VLQ generating the *Yukawa operators*, always generate the *Derivative operators*, and therefore are subject to strong constraints. Therefore, in the following we focus on the simplest scalar scenario generating the *Yukawa operators*: topology A, the Two-Higgs-Doublet Model.

3 The general (Type III) Two-Higgs-Doublet Model

In this section we introduce the general 2HDM, also known as Type III 2HDM. Reviews addressing different 2HDMs can be found in refs. [32, 53–56]. In section 3.1 we discuss the scalar potential and in section 3.2 the Yukawa couplings. Aspects relevant for Higgs flavor-changing processes are studied in section 3.2.1.

3.1 The scalar potential

In a generic basis both Higgs scalar doublets Φ_1 and Φ_2 take VEVs denoted by v_1 and v_2, respectively. One can rotate to the Higgs basis [57–59] where only one linear combination of Φ_1 and Φ_2, denoted by H_1, has a non-vanishing VEV, equal to $v = \sqrt{v_1^2 + v_2^2} \simeq 246\,\text{GeV}$, via the transformation

$$\begin{pmatrix} H_1 \\ H_2 \end{pmatrix} = \begin{pmatrix} c_\beta & s_\beta \\ -s_\beta & c_\beta \end{pmatrix} \begin{pmatrix} \Phi_1 \\ \Phi_2 \end{pmatrix} , \tag{3.1}$$

where the angle β defines the mixing between the two doublets, with $\tan\beta \equiv v_2/v_1$, and the short-hand notations $s_x \equiv \sin x$ and $c_x \equiv \cos x$. We will also use $t_x \equiv \tan x$. In the Higgs basis, the doublets take the form

$$H_1 = \begin{pmatrix} G^+ \\ \frac{1}{\sqrt{2}}\left(v + \varphi_1 + iG^0\right) \end{pmatrix} , \qquad H_2 = \begin{pmatrix} H^+ \\ \frac{1}{\sqrt{2}}\left(\varphi_2 + iA\right) \end{pmatrix} , \tag{3.2}$$

where φ_1 and φ_2 are CP-even neutral Higgs fields, A is a CP-odd neutral Higgs field, H^+ is a charged Higgs field, and G^+ and G^0 are the would-be Goldstone bosons, which provide the longitudinal polarizations of the W^+ and the Z gauge bosons. The most general scalar potential is given in the Higgs basis by[2]

$$\begin{aligned} V = {} & M_{11}^2 H_1^\dagger H_1 + M_{22}^2 H_2^\dagger H_2 - \left(M_{12}^2 H_2^\dagger H_1 + \text{H.c.}\right) + \frac{1}{2}\Lambda_1 \left(H_1^\dagger H_1\right)^2 \\ & + \frac{1}{2}\Lambda_2 \left(H_2^\dagger H_2\right)^2 + \Lambda_3 \left(H_1^\dagger H_1\right)\left(H_2^\dagger H_2\right) + \Lambda_4 \left(H_1^\dagger H_2\right)\left(H_2^\dagger H_1\right) \\ & + \left\{\frac{1}{2}\Lambda_5 \left(H_1^\dagger H_2\right)^2 + \left[\Lambda_6 \left(H_1^\dagger H_1\right) + \Lambda_7 \left(H_2^\dagger H_2\right)\right] H_1^\dagger H_2 + \text{H.c.}\right\} , \end{aligned} \tag{3.3}$$

where Λ_i $(i = 1, 2, \ldots, 7)$ are the quartic couplings and M_{ij}^2 are bare mass-squared parameters. In general, Λ_5, Λ_6, Λ_7 and M_{12} can be complex but, by redefining H_1 and H_2, one

[2]The transformations of parameters between different scalar bases can be found in appendix A of ref. [54].

JHEP02(2020)147

can, for example, choose Λ_5 to be real [54]. We assume, for simplicity, a CP conserving scalar sector: all the parameters in eq. (3.3) are real.

The minimisation conditions

$$M_{11}^2 = -\frac{1}{2}\Lambda_1 v^2\,, \qquad M_{12}^2 = \frac{1}{2}\Lambda_6 v^2\,, \tag{3.4}$$

can be used to eliminate M_{11}^2 and M_{12}^2 as independent parameters. Inserting $\langle H_1\rangle = (0, v/\sqrt{2})^T$ into eq. (3.3), we obtain the squared mass of the charged scalar,

$$m_{H^\pm}^2 = M_{22}^2 + \frac{1}{2}v^2\Lambda_3\,, \tag{3.5}$$

and the mass matrix of the CP-even neutral scalars

$$\mathcal{M}_h^2 = \begin{pmatrix} \Lambda_1 v^2 & \Lambda_6 v^2 \\ \Lambda_6 v^2 & m_A^2 + \Lambda_5 v^2 \end{pmatrix}\,, \tag{3.6}$$

where the mass of the CP-odd scalar is

$$m_A^2 = m_{H^\pm}^2 - \frac{1}{2}v^2\left(\Lambda_5 - \Lambda_4\right)\,. \tag{3.7}$$

Thus, in the Higgs basis, the mass eigenstates h and H are a mixture of the CP-even states φ_1 and φ_2

$$\begin{pmatrix} h \\ H \end{pmatrix} = \begin{pmatrix} s_{\beta-\alpha} & c_{\beta-\alpha} \\ c_{\beta-\alpha} & -s_{\beta-\alpha} \end{pmatrix} \begin{pmatrix} \varphi_1 \\ \varphi_2 \end{pmatrix}\,, \tag{3.8}$$

with masses

$$m_{H,h}^2 = \frac{1}{2}\left\{ m_A^2 + v^2\left(\Lambda_1 + \Lambda_5\right) \pm \sqrt{\left[m_A^2 + v^2\left(\Lambda_5 - \Lambda_1\right)\right]^2 + 4v^4\Lambda_6^2} \right\}\,. \tag{3.9}$$

The mixing in eq. (3.8) is

$$s_{2(\beta-\alpha)} = -\frac{2\Lambda_6 v^2}{m_H^2 - m_h^2}. \tag{3.10}$$

It will turn out useful to obtain Λ_6 by combining eqs. (3.9) and (3.10)

$$\Lambda_6 = \frac{t_{2(\beta-\alpha)}}{2v^2}\left[m_A^2 + v^2(\Lambda_5 - \Lambda_1) \right]. \tag{3.11}$$

Eq. (3.10) and eq. (3.11) determine the sign of Λ_6 in terms of $\beta - \alpha$. In the general 2HDM t_β is not a physical parameter (see ref. [60] for a complete discussion regarding the significance of t_β). On the contrary, $s_{\beta-\alpha}$ is a physical quantity; it needs to be sufficiently close to one (i.e., in the alignment or in the decoupling limit) so h is an adequately SM-like Higgs boson, in agreement with current observations. In this limit $t_{2(\beta-\alpha)}$, and thus Λ_6, approach zero (for $\Lambda_6 = 0$ h is exactly SM-like, with $m_h^2 = \Lambda_1 v^2$, see eq. (3.9)).

JHEP02(2020)147

3.2 The Yukawa Lagrangian

In order to have HQFV, both scalar doublets must couple to the quarks. The most general Yukawa Lagrangian in the generic scalar basis $\{\Phi_1, \Phi_2\}$ reads

$$-\mathcal{L}_Q = \bar{Q}^0 \left(Y_{u1}^\dagger \tilde{\Phi}_1 + Y_{u2}^\dagger \tilde{\Phi}_2\right) u_{\mathrm{R}}^0 + \bar{Q}^0 \left(Y_{d1}^\dagger \Phi_1 + Y_{d2}^\dagger \Phi_2\right) d_{\mathrm{R}}^0 + \mathrm{H.c.}\,. \tag{3.12}$$

Y_{d1}, Y_{d2}, Y_{u1} and Y_{u2} are completely general 3×3 complex Yukawa matrices (generation indices are, again, understood and omitted). The lepton sector is assumed to be SM-like. The quark mass matrices are given by

$$M_U = \frac{v}{\sqrt{2}} \left(c_\beta Y_{u1}^\dagger + s_\beta Y_{u2}^\dagger\right), \qquad M_D = \frac{v}{\sqrt{2}} \left(c_\beta Y_{d1}^\dagger + s_\beta Y_{d2}^\dagger\right). \tag{3.13}$$

We can rotate $\{\Phi_1, \Phi_2\}$ into the Higgs basis

$$-\mathcal{L}_Q = \bar{Q}^0 \left[\frac{\sqrt{2} M_U}{v} \tilde{H}_1 + \xi^U \tilde{H}_2\right] u_{\mathrm{R}}^0 + \bar{Q}^0 \left[\frac{\sqrt{2} M_D}{v} H_1 + \xi^D H_2\right] d_{\mathrm{R}}^0 + \mathrm{H.c.}\,, \tag{3.14}$$

where

$$\xi^D \equiv \frac{Y_{d2}^\dagger}{c_\beta} - \frac{\sqrt{2} t_\beta M_D}{v}, \qquad \xi^U \equiv \frac{Y_{u2}^\dagger}{c_\beta} - \frac{\sqrt{2} t_\beta M_U}{v}. \tag{3.15}$$

Rotating the quark fields into the mass eigenstate bases u_a and d_a (without "0" superscripts), $M_Q \mapsto D_{\mathrm{q}}$ and $\xi^Q \mapsto \hat{\xi}^Q$; without loss of generality we may work, as in section 2, in a basis where M_U is diagonal with real and positive elements m_u, m_c, and m_t. Then, the Yukawa lagrangian reads

$$\begin{aligned}
-\mathcal{L}_Q = {} & \bar{u}_b \left(V_{bc}\, \hat{\xi}_{ca}^D P_R - \hat{\xi}_{cb}^{U*} V_{ca} P_L\right) d_a\, H^+ \\
& + \bar{d}_b \left(\hat{\xi}_{cb}^{D*} V_{ac}^* P_L - V_{cb}^* \hat{\xi}_{ca}^U P_R\right) u_a\, H^- \\
& + \Bigg(\bar{d}_b \left[\left\{\frac{D_{\mathrm{d},ba}}{v} s_{\beta-\alpha} + \frac{1}{\sqrt{2}} \hat{\xi}_{ba}^D c_{\beta-\alpha}\right\} P_R + \left\{\frac{D_{\mathrm{d},ba}}{v} s_{\beta-\alpha} + \frac{1}{\sqrt{2}} \hat{\xi}_{ba}^{D*} c_{\beta-\alpha}\right\} P_L\right] d_a \\
& + \bar{u}_b \left[\left\{\frac{D_{\mathrm{u},ba}}{v} s_{\beta-\alpha} + \frac{1}{\sqrt{2}} \hat{\xi}_{ba}^U c_{\beta-\alpha}\right\} P_R + \left\{\frac{D_{\mathrm{u},ba}}{v} s_{\beta-\alpha} + \frac{1}{\sqrt{2}} \hat{\xi}_{ba}^{U*} c_{\beta-\alpha}\right\} P_L\right] u_a\Bigg) h \\
& + \Bigg(\bar{d}_b \left[\left\{\frac{D_{\mathrm{d},ba}}{v} c_{\beta-\alpha} - \frac{1}{\sqrt{2}} \hat{\xi}_{ba}^D s_{\beta-\alpha}\right\} P_R + \left\{\frac{D_{\mathrm{d},ba}}{v} c_{\beta-\alpha} - \frac{1}{\sqrt{2}} \hat{\xi}_{ba}^{D*} s_{\beta-\alpha}\right\} P_L\right] d_a \\
& + \bar{u}_b \left[\left\{\frac{D_{\mathrm{u},ba}}{v} c_{\beta-\alpha} - \frac{1}{\sqrt{2}} \hat{\xi}_{ba}^U s_{\beta-\alpha}\right\} P_R + \left\{\frac{D_{\mathrm{u},ba}}{v} c_{\beta-\alpha} - \frac{1}{\sqrt{2}} \hat{\xi}_{ba}^{U*} s_{\beta-\alpha}\right\} P_L\right] u_a\Bigg) H \\
& + \frac{i}{\sqrt{2}} \left(\bar{d}_b \left[\hat{\xi}_{ba}^D P_R - \hat{\xi}_{ba}^{D*} P_L\right] d_a + \bar{u}_b \left[-\hat{\xi}_{ba}^U P_R + \hat{\xi}_{ba}^{U*} P_L\right] u_a\right) A\,,
\end{aligned} \tag{3.16}$$

where $a, b = 1, 2, 3$. The correspondence with the notation in ref. [35], for a generic Yukawa coupling

$$\bar{q}_b\, g_{\bar{q}_b q_a \phi}\, q_a\, \phi \equiv \bar{q}_b \left(\Gamma_{q_b q_a}^{LR\,\phi} P_R + \Gamma_{q_b q_a}^{RL\,\phi} P_L\right) q_a\, \phi\,, \tag{3.17}$$

JHEP02(2020)147

	$\Gamma^{LR\phi}_{q_b q_a}$	$\Gamma^{RL\phi}_{q_b q_a}$
$\bar{q}_b q_a h$	$\frac{D_{\mathrm{q},ba}}{v} s_{\beta-\alpha} + \frac{1}{\sqrt{2}} \hat{\xi}^Q_{ba} c_{\beta-\alpha}$	$\frac{D_{\mathrm{q},ba}}{v} s_{\beta-\alpha} + \frac{1}{\sqrt{2}} (\hat{\xi}^Q_{ba})^* c_{\beta-\alpha}$
$\bar{q}_b q_a H$	$\frac{D_{\mathrm{q},ba}}{v} c_{\beta-\alpha} - \frac{1}{\sqrt{2}} \hat{\xi}^Q_{ba} s_{\beta-\alpha}$	$\frac{D_{\mathrm{q},ba}}{v} c_{\beta-\alpha} - \frac{1}{\sqrt{2}} (\hat{\xi}^Q_{ba})^* s_{\beta-\alpha}$
$\bar{q}_b q_a A$	$\frac{i}{\sqrt{2}} \hat{\xi}^Q_{ba}$	$-\frac{i}{\sqrt{2}} (\hat{\xi}^Q_{ba})^*$
$\bar{u}_b d_a H^+$	$V_{bc}\, \hat{\xi}^D_{ca}$	$-(\hat{\xi}^U_{cb})^*\, V_{ca}$

Table 4. Scalar-quark-quark couplings extracted from eq. (3.16) using the convention of eq. (3.17), where $Q = D, U$.

where $P_{R,L} = (1 \pm \gamma_5)/2$, is provided in table 4. Due to Hermiticity of the Lagrangian, $\Gamma^{LR\phi\,*}_{q_a q_b} = \Gamma^{RL\phi}_{q_b q_a}$.

In this work we are interested in HQFV involving a third family quark. Therefore we will only consider the flavor-violating (complex) couplings in $\hat{\xi}^{U,\,D}$ between the third and the second families, and in addition for simplicity we set the diagonal coupling of the second generation to zero, that is,

$$\hat{\xi}^U = \begin{pmatrix} 0 & 0 & 0 \\ 0 & 0 & \hat{\xi}^U_{23} \\ 0 & \hat{\xi}^U_{32} & \hat{\xi}^U_{33} \end{pmatrix}, \qquad \hat{\xi}^D = \begin{pmatrix} 0 & 0 & 0 \\ 0 & 0 & \hat{\xi}^D_{23} \\ 0 & \hat{\xi}^D_{32} & \hat{\xi}^D_{33} \end{pmatrix}. \tag{3.18}$$

The only a priori requirement placed on the entries of $\hat{\xi}^U$ and $\hat{\xi}^D$ is that they respect perturbativity, i.e. they are smaller than 4π.

3.2.1 Flavor-changing Higgs processes

In eq. (3.16), $\mathcal{L}_Q$ includes flavor-changing couplings of h to $\bar{b}s$, $\bar{s}b$, $\bar{t}c$ and $\bar{c}t$ controlled by the off-diagonal entries of $\hat{\xi}^U$ and $\hat{\xi}^D$ in eq. (3.18). The $h \to bs$ decay width at tree-level, $\Gamma(h \to bs) \equiv \Gamma(h \to \bar{b}s) + \Gamma(h \to \bar{s}b)$, is

$$\Gamma(h \to bs) \simeq \frac{3 m_h c^2_{\beta-\alpha}}{16\pi} \left(|\hat{\xi}^D_{23}|^2 + |\hat{\xi}^D_{32}|^2 \right), \tag{3.19}$$

where we have neglected final state masses. The $t \to ch$ decay width at tree-level reads

$$\Gamma(t \to ch) \simeq \frac{m_t c^2_{\beta-\alpha}}{32\pi} |\hat{\xi}^U_{32}|^2 \left(1 - \frac{m_h^2}{m_t^2} \right)^2, \tag{3.20}$$

where we have neglected the charm mass. For the conjugate process $\bar{t} \to h\bar{c}$, $\hat{\xi}^U_{32} \mapsto \hat{\xi}^U_{23}$.

In the analysis of section 5, scalar decays are carried out using the inbuilt routines offered by 2HDMC [61]. The 2HDMC code does not support flavor-changing processes officially but the program is designed thoughtfully to allow for these processes. Nevertheless, some slight modifications had to be made, including promoting the Yukawa entries from real to complex. Furthermore, beyond eq. (3.19), $h \to bs$ receives QCD corrections at NLO that may increase the rate by 10–20% [29]. The 2HDMC includes QCD corrections for this process, and they are turned on in the analysis of section 5.

JHEP02(2020)147

3.3 General constraints on the 2HDM

3.3.1 Constraints on quartic couplings

Since the Hamiltonian has to be bounded from below, the quartic part of the scalar potential in eq. (3.3) is required to be positive for all values of the fields and all scales. Furthermore, the considered vacuum should be the global minimum of the potential [62] (one could weaken the requirement and include a sufficiently long-lived metastable local minimum). The quartic couplings are also required to be perturbative, i.e. smaller than 4π. We also require that the scattering of the different scalars at high energies, controlled by the quartic part of the potential, respects perturbative unitarity: in particular, that the eigenvalues of the tree-level $2 \to 2$ scattering matrix do not yield probabilities larger than 1 (see e.g. [63–65], one loop corrections in a restricted 2HDM have been addressed in ref. [66]).

3.3.2 Oblique parameters

We include the so-called "oblique parameters" S, T and U [67, 68], which parametrise radiative corrections to electroweak gauge boson propagators. For the theoretical expressions, see refs. [69, 70]; we use the experimental values [71]

$$S = 0.05 \pm 0.11, \;\; T = 0.09 \pm 0.13, \;\; U = 0.01 \pm 0.11, \tag{3.21}$$

with a correlation matrix

$$\Sigma_{S,T,U} = \begin{pmatrix} 1.0 & 0.9 & -0.59 \\ 0.9 & 1.0 & -0.83 \\ -0.59 & -0.83 & 1.0 \end{pmatrix} . \tag{3.22}$$

3.3.3 Higgs signal strengths

A necessary ingredient in the scalar sector is, of course, a neutral scalar with properties in agreement with the 125 GeV SM-like Higgs discovered at the LHC [1, 2]. We identify it with h, and thus the first requirement is $m_h = (125.09 \pm 0.32)\,\text{GeV}$ [72]. The width is also required to satisfy $\Gamma_h < 17\,\text{MeV}$ following the result at 2σ presented in ref. [73]. The most relevant information for the phenomenological aspects of the 125 GeV scalar is the set of signal strengths μ_{XY} for combined production (Y) and decay (X) channels

$$\mu_{XY} = \frac{\sigma([pp]_Y \to h)_{\text{2HDM}}\,\text{BR}(h \to X)_{\text{2HDM}}}{\sigma([pp]_Y \to h)_{\text{SM}}\,\text{BR}(h \to X)_{\text{SM}}} , \tag{3.23}$$

which are factorized in "production $\times$ decay" model dependent factors

$$\mu_{XY} = \kappa_Y^P \kappa_X^{BR}, \qquad \kappa_Y^P = \frac{\sigma([pp]_Y \to h)_{\text{2HDM}}}{\sigma([pp]_Y \to h)_{\text{SM}}}, \quad \kappa_X^{BR} = \frac{\text{BR}(h \to X)_{\text{2HDM}}}{\text{BR}(h \to X)_{\text{SM}}} . \tag{3.24}$$

The relevant production modes are gluon-gluon fusion (ggF), vector boson fusion (VBF), Higgs-strahlung (Wh, Zh) and associated production with top quarks (tth); the corresponding factors are

$$\kappa_{tth}^P = \frac{v^2}{2m_t^2}\left(|\Gamma_{tt}^{LRh}|^2 + |\Gamma_{tt}^{RLh}|^2\right) ,$$

$$\kappa_{ggF}^P = \frac{\Gamma(h \to gg)_{\text{2HDM}}}{\Gamma(h \to gg)_{\text{SM}}} , \qquad \kappa_{VBF}^P = \kappa_{WH}^P = \kappa_{ZH}^P = s_{\beta-\alpha}^2 . \tag{3.25}$$

JHEP02(2020)147

The corresponding factors for the relevant decay channels are

$$\kappa_{bb}^{BR} = \frac{v^2}{2m_b^2}\left(|\Gamma_{bb}^{LRh}|^2 + |\Gamma_{bb}^{RLh}|^2\right), \qquad \kappa_{\tau\tau}^{BR} = \frac{v^2}{2m_\tau^2}\left(|\Gamma_{\tau\tau}^{LRh}|^2 + |\Gamma_{\tau\tau}^{RLh}|^2\right),$$
$$\kappa_{\gamma\gamma}^{BR} = \frac{\Gamma(h\to\gamma\gamma)_{\rm 2HDM}}{\Gamma(h\to\gamma\gamma)_{\rm SM}}, \qquad \kappa_{WW}^{BR} = \kappa_{ZZ}^{BR} = s_{\beta-\alpha}^2 . \tag{3.26}$$

Both κ_{ggF}^{P} and $\kappa_{\gamma\gamma}^{BR}$ arise from one loop amplitudes: the expressions can be found, for example, in ref. [74]. For $h \to \bar{\tau}\tau$, since we assume for simplicity SM-like Yukawa couplings in the lepton sector, $\kappa_{\tau\tau}^{BR} = s_{\beta-\alpha}^2$ (the experimental uncertainties in that decay channel are, in any case, large).

The experimental results (values and uncertainties) from the combined ATLAS and CMS analyses of LHC Run I data [75] are given in the following matrix:

$$\mu_{XY} = \begin{pmatrix} 1.1^{+0.23}_{-0.22} & 1.3^{+0.5}_{-0.5} & 0.5^{+1.3}_{-1.2} & 0.5^{+3.0}_{-2.5} & 2.2^{+1.6}_{-1.3} \\ 1.13^{+0.23}_{-0.22} & 0.1^{+0.5}_{-0.5} & \times & \times & \times \\ 0.84^{+0.17}_{-0.17} & 1.2^{+0.4}_{-0.4} & 1.6^{+1.2}_{-1.0} & 5.9^{+2.6}_{-2.2} & 5.0^{+1.8}_{-1.7} \\ 1.0^{+0.6}_{-0.6} & 1.3^{+0.4}_{-0.4} & -1.4^{+1.4}_{-1.4} & 2.2^{+2.2}_{-1.8} & -1.9^{+3.7}_{-3.3} \\ \times & \times & 1.0^{+0.5}_{-0.5} & 0.4^{+0.4}_{-0.4} & 1.1^{+1.0}_{-1.0} \end{pmatrix}. \tag{3.27}$$

The ordering for decay channels (rows) is $\{\gamma\gamma, ZZ, WW, \tau\tau, bb\}$ and for production mechanisms (columns) {ggF, VBF, Wh, Zh, tth}. For the missing entries "×" there is no measurement available in ref. [75]. In addition to eq. (3.27), we also include CMS and ATLAS data from LHC Run II on $h \to \bar{b}b$ and $h \to \bar{\tau}\tau$ in the analysis of section 5: for $h \to \bar{b}b$, we consider CMS [76] and ATLAS [77] results for VBF production while for $h \to \bar{\tau}\tau$ we combine ggF and VBF production following ref. [78]. Notice that the analysis of Higgs signal strengths only requires the 2HDM vs. SM modifying factors in eqs. (3.25)–(3.26).

4 Flavor constraints

In order to study HQFV in the general 2HDM, flavor constraints have to be included. We discuss the most relevant constraints in the following.

In the down quark sector we focus on the process $h \to bs$: in this case, the most stringent constraints come from the $|\Delta B| = 2$ process of B_s^0–$\bar{B}_s^0$ mixing and from the $|\Delta B| = 1$ radiative decay process $B \to X_s\gamma$. Since in the SM all flavor-changing processes are induced by W boson exchange, both processes occur at the one loop-level. Their GIM and loop suppressions make them highly sensitive to the presence of new physics contributions: in the general 2HDM these new contributions appear at tree-level in B_s^0–$\bar{B}_s^0$ and at one loop in $B \to X_s\gamma$. They are discussed in the following subsections. We do not consider other processes involving final state leptons like, e.g., $B_s \to \mu^+\mu^-$: since we focus on the quark sector, assuming SM-like tree-level couplings of scalars to leptons highly suppresses new contributions to these processes.

JHEP02(2020)147

Concerning HQFV in the up quark sector, as already mentioned, we focus on $t \to ch$: we incorporate existing bounds at the 10^{-3} level on $\mathrm{BR}(t \to ch)$ (see eq. (1.1)). One could also consider constraints arising from D^0–$\bar{D}^0$ mixing. However, with the Yukawa couplings considered in eq. (3.18), the contribution to D^0–$\bar{D}^0$ mixing involving $\hat{\xi}^U$ vanishes.[3] We do not consider constraints from $t \to cg, c\gamma$ processes since in this scenario they only arise at one loop while existing bounds on the corresponding branching ratios are similar to the ones for $t \to ch$, which arise instead at tree-level.

4.1 Effective operators

We use an Effective Field Theory (EFT) approach to compute flavor constraints. An effective Hamiltonian is defined as

$$\mathcal{H}_{\text{eff}} = (\text{PF}) \sum_i C_i(\mu)\, O_i(\mu), \tag{4.1}$$

where μ is the energy scale at which the matrix elements of the Hamiltonian are evaluated, $C_i(\mu)$ are the Wilson coefficients which encode the information of the underlying theory and $O_i(\mu)$ are the operators which mediate the process. For simplicity it is common to include powers of the weak coupling or CKM factors in the prefactor (PF): for example, for $b \to s$ transitions, it is common to set $(\text{PF}) = -\frac{4G_F}{\sqrt{2}} V_{ts}^* V_{tb}$.

The underlying theory and the EFT are typically matched at an energy scale $\mu \sim m_W$: the evolution ("running") of the Wilson coefficients from the matching scale down to the B meson scale $\mu_B \sim 4.2\,\text{GeV}$ is given by

$$\frac{d}{d\ln\mu} C_i(\mu) = \gamma_{ji} C_j(\mu), \tag{4.2}$$

where γ_{ij} is the anomalous dimension matrix (ADM). The solution of this Renormalization Group Evolution equation, in vector notation, is given by

$$\vec{C}(\mu) = \hat{U}(\mu, \mu_0)\vec{C}(\mu_0), \tag{4.3}$$

where the evolution operator matrix $\hat{U}(\mu, \mu_0)$ is computed in terms of γ_{ji} [80] and can be found using the publicly available Mathematica code DSixTools [81], see also ref. [82].

4.2 B_s^0–$\bar{B}_s^0$ meson mixing

In neutral meson systems M^0–$\bar{M}^0$, $M^0 \leftrightarrows \bar{M}^0$ transitions (or "oscillations") show that M^0 and $\bar{M}^0$ are not evolution eigenstates; the evolution eigenstates have slightly different mass and width. In the B_s^0–$\bar{B}_s^0$ system, the physical mass splitting ΔM_{B_s} is dominated

[3] There are one loop contributions mediated by the charged scalar which depend on $\hat{\xi}^D$, but they are irrelevant once the constraints from the down quark sector discussed above are considered. Notice, in any case, that while B_s^0–$\bar{B}_s^0$ transitions are dominated by short-distance physics (e.g. the contributions mediated by the top quark), long-distance effects (i.e. intermediate hadronic states) are quite likely dominating in D^0–$\bar{D}^0$ and only a rough constraint on the size of the short-distance scalar mediated contributions could have been considered.

JHEP02(2020)147

by short-distance physics and can be computed perturbatively in terms of the appropriate effective hamiltonian

$$M_{12}^{B_s} = \frac{\langle B_s^0|\mathcal{H}_{\rm eff}^{|\Delta B|=2}|\bar{B}_s^0\rangle}{2M_{B_s}}, \qquad \Delta M_{B_s} = 2|M_{12}^{B_s}|\,. \tag{4.4}$$

The CP violating mixing phase is[4]

$$2\beta_s = -\arg\left(\langle B_s^0|\mathcal{H}_{\rm eff}^{|\Delta B|=2}|\bar{B}_s^0\rangle\right)\,. \tag{4.5}$$

In the EFT description of B_s^0–$\bar{B}_s^0$ mixing, we adopt the usual operator basis:

$$\begin{aligned} O_1 &= (\bar{s}_\alpha\gamma^\mu P_L b_\alpha)(\bar{s}_\beta\gamma^\mu P_L b_\beta),\\ O_2 &= (\bar{s}_\alpha P_L b_\alpha)(\bar{s}_\beta P_L b_\beta),\\ O_3 &= (\bar{s}_\alpha P_L b_\beta)(\bar{s}_\beta P_L b_\alpha),\\ O_4 &= (\bar{s}_\alpha P_L b_\alpha)(\bar{s}_\beta P_R b_\beta),\\ O_5 &= (\bar{s}_\alpha P_L b_\beta)(\bar{s}_\beta P_R b_\alpha), \end{aligned} \tag{4.6}$$

where we have explicitly denoted the color indices α and β. Exchanging $P_L \leftrightarrows P_R$ in $O_{1,2,3}$ one obtains the (additional) primed operators $O'_{1,2,3}$ ($O_{4,5}$ do not give new operators under $P_L \leftrightarrows P_R$). The full Hamiltonian describing B_s^0–$\bar{B}_s^0$ is

$$\mathcal{H}_{\rm eff}^{|\Delta B|=2} = \sum_{i=1}^{5} C_i(\mu)O_i(\mu) + \sum_{i=1}^{3} C'_i(\mu)O'_i(\mu). \tag{4.7}$$

Since, as discussed below, W mediated contributions only affect C_1, while the new scalar contributions affect C_2, C_2' and C_4, we do not factor out the usual G_F and $(V_{ts}^*V_{tb})^2$ in eq. (4.7). For the B_s system

$$\langle B_s^0|\mathcal{H}_{\rm eff}^{|\Delta B|=2}|\bar{B}_s^0\rangle = \sum_{i=1}^{5} C_i(\mu)\,\langle B_s^0|O_i(\mu)|\bar{B}_s^0\rangle + \sum_{i=1}^{3} C'_i(\mu)\,\langle B_s^0|O'_i(\mu)|\bar{B}_s^0\rangle, \tag{4.8}$$

the matrix elements of the operators in eq. (4.6) are

$$\begin{aligned} \langle B_s^0|O_1(\mu)|\bar{B}_s^0\rangle &= b_1\, M_{B_s}^2 f_{B_s}^2 B_1^{B_s}(\mu),\\ \langle B_s^0|O_i(\mu)|\bar{B}_s^0\rangle &= b_i\,\chi_{B_s}\, M_{B_s}^2 f_{B_s}^2 B_i^{B_s}(\mu), \qquad i=2,3,4,5, \end{aligned} \tag{4.9}$$

$$\vec{b} = \{8/3,\ -5/3,\ 1/3,\ 2,\ 2/3\}\,, \qquad \chi_{B_s}(\mu) = \frac{M_{B_s}^2}{(m_b(\mu)+m_s(\mu))^2}\,. \tag{4.10}$$

Non-perturbative QCD effects [83] are encoded in the bag factors $B_i^{B_s}$ (the vacuum insertion approximation corresponds to $B_i^{B_s}\to 1$); they are given in table 9 in appendix B, together with the decay constant f_{B_s} and the meson mass M_{B_s}. The primed operators of appendix C have the same matrix elements as the unprimed ones (from parity invariance of QCD).

[4]Notice that the mixing phase is not rephasing invariant and thus it is only its combination with decay amplitudes which has a rephasing invariant physical meaning; as is usual, we refer nevertheless to the "mixing phase" $2\beta_s$ since, in the adopted CKM phase convention, one has real decay amplitudes in transitions like the "golden" mode $B_s \to J/\Psi\,\phi$.

JHEP02(2020)147

4.2.1 Standard model contribution

As anticipated, in the SM there are only contributions to the O_1 operator. The dominant contribution to C_1 (see figure 4a) is

$$C_1^{\rm SM}(\mu_B) = \frac{G_F^2}{4\pi^2}\left(V_{ts}^* V_{tb}\right)^2 m_W^2 \hat{\eta}_B(\mu_B) S(x_t)\,, \quad x_t \equiv m_t^2/m_W^2\,, \tag{4.11}$$

with $S(x)$ the well-known Inami-Lim function [84]. The RGE for $\Delta F = 2$ is given in appendix C: one can read the evolution of C_1 from the matching scale $\mu_W \sim m_W$ down to $\mu_B \sim m_B$, given by $\hat{\eta}_B(\mu_B) = 0.862$. Then

$$\langle B_s^0|\mathcal{H}_{\rm eff}^{|\Delta B|=2}|\bar{B}_s^0\rangle = \frac{G_F^2 m_W^2}{6\pi^2} M_{B_s}^2 f_{B_s}^2 \hat{\eta}_B B_1^{B_s}\left(V_{ts}^* V_{tb}\right)^2 S(x_t)\,. \tag{4.12}$$

Individually, the evolution factor $\hat{\eta}_B$ and bag-factor $B_1^{B_s}$ are both scale dependent, but the combination of $\hat{\eta}_B B_1^{B_s}$ is a scale as well as scheme-independent quantity. Numerically

$$\langle B_s^0|\mathcal{H}_{\rm eff}^{|\Delta B|=2}|\bar{B}_s^0\rangle_{\rm SM} = (7.28 - 0.26i) \times 10^{-11}\,\text{GeV}, \tag{4.13}$$

which gives

$$\Delta M_{B_s,\,\rm SM} = (1.36 \pm 0.08) \times 10^{-11}\,\text{GeV} = (20.64 \pm 1.28)\,\text{ps}^{-1}\,. \tag{4.14}$$

The theoretical error we choose is based upon the combination of QCD errors as laid out in table II of ref. [85], where a theoretical error of 6.2% is stated. Using $\hat{\eta}_B = 0.839$ (see refs. [86, 87]), $\Delta M_{B_s,\,\rm SM}$ agrees with ref. [85]. We have updated our final scan and predictions with this improved quantity, which gives $\Delta M_{B_s,\,\rm SM} = 1.32 \times 10^{-11}\,\text{GeV}$. The SM final value in eq. (4.14) is larger than the observed one, specifically, its error translates into a 1.8σ discrepancy with the SM, as alluded to in ref. [85]. The B_s^0–$\bar{B}_s^0$ mixing phase reads

$$\beta_{s,\,\rm SM} = (1.82 \pm 0.11) \times 10^{-2}\,\text{rad}\,. \tag{4.15}$$

In table 5 we summarize the values observed and computed for the SM.

4.2.2 Two-Higgs-Doublet Model contributions

At tree-level, the B_s^0–$\bar{B}_s^0$ mixing process is mediated by neutral scalars h, H and A, as shown in figure 4b. The contributions to the Wilson Coefficients are [35]

$$\begin{aligned}
C_2(\mu_W) &= \sum_{k=1}^{3} -\frac{1}{2m_{\phi_k^0}^2}\left(\Gamma_{32}^{LR,\phi_k^0\star}\right)^2\,,\\
C_2'(\mu_W) &= \sum_{k=1}^{3} -\frac{1}{2m_{\phi_k^0}^2}\left(\Gamma_{23}^{LR,\phi_k^0}\right)^2\,,\\
C_4(\mu_W) &= \sum_{k=1}^{3} -\frac{1}{m_{\phi_k^0}^2}\Gamma_{23}^{LR,\phi_k^0}\Gamma_{32}^{LR,\phi_k^0\star}\,,
\end{aligned} \tag{4.16}$$

where $\phi_k^0 = (h, H, A)$. Beyond tree-level, there are contributions from neutral and charged scalar particles from box diagrams as shown in figures 4c and 4d; for the corresponding expressions we refer to ref. [35].

JHEP02(2020)147

Observable	Value
$\Delta M_{B_s,\,\mathrm{obs}}$	$(1.1688 \pm 0.0014) \times 10^{-11}\,\mathrm{GeV}$ [16]
$\Delta M_{B_s,\,\mathrm{SM}}$	$(1.32 \pm 0.08_{\mathrm{th.}}) \times 10^{-11}\,\mathrm{GeV}$
$\beta_{s,\,\mathrm{obs}}$	$(1.5 \pm 1.6) \times 10^{-2}\,\mathrm{rad}$ [16]
$\beta_{s,\,\mathrm{SM}}$	$(1.82 \pm 0.11_{\mathrm{th.}}) \times 10^{-2}\,\mathrm{rad}$
$\mathrm{BR}(B \to X_s\gamma)_{\mathrm{obs}}$	$(3.32 \pm 0.16) \times 10^{-4}$ [79]
$\mathrm{BR}(B \to X_s\gamma)_{\mathrm{SM}}$	$(3.34 \pm 0.33_{\mathrm{th.}}) \times 10^{-4}$

Table 5. Experimental and SM predictions for B_s-meson mixing observables (mass splitting and the CP violating angle) and radiative B-meson decays. The subscript *th.* in some errors refers to theoretical.

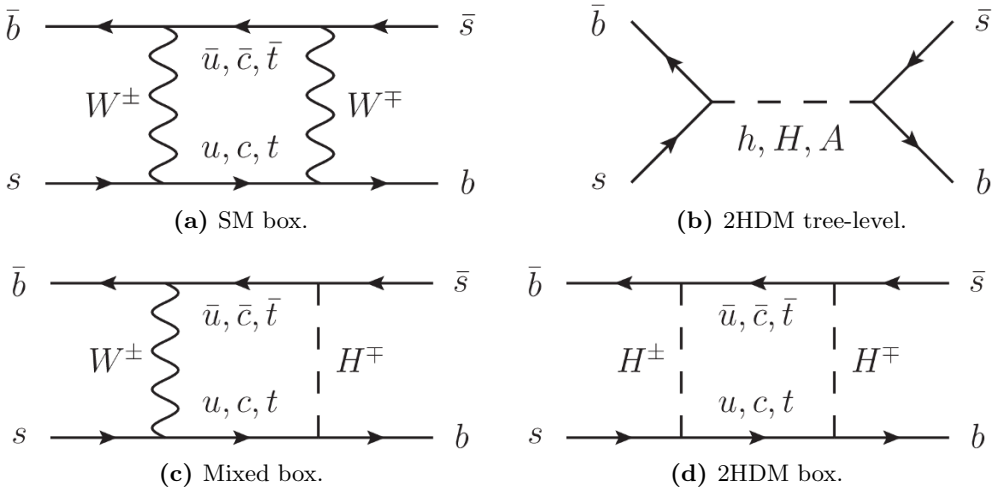

(a) SM box. **(b)** 2HDM tree-level. **(c)** Mixed box. **(d)** 2HDM box.

Figure 4. Contributions to B_s^0–$\bar{B}_s^0$ mixing.

4.2.3 Explaining the discrepancy within the Two-Higgs-Doublet Model

Before addressing the full numerical analysis of section 5, it is interesting to study the parameter space in the 2HDM that can explain the 1.8σ deviation between the observed value of ΔM_{B_s} and the SM prediction, see table 5. Notice that the 2HDM contribution can partially cancel the SM contribution, and therefore yield a better agreement with the lower observed value. For degenerate H and A as expected from EWPT, the tree-level contributions to the Wilson coefficients in eq. (4.16) give

$$\begin{aligned}
&\Delta M_{B_s,\,\mathrm{2HDM\ tree\text{-}level}} \\
&= C_2(\mu_b)\langle O_2\rangle + C_2'(\mu_b)\langle O_2\rangle + C_4'(\mu_b)\langle O_4\rangle, \\
&= -A_B\Bigg\{\frac{1}{4}c_{\beta-\alpha}^2\left[\frac{1}{m_h^2}-\frac{1}{m_H^2}\right]\Big((U_{22}B_2^{B_s}b_2 + U_{32}B_3^{B_s}b_3)(\hat{\xi}_{32}^{D\star\,2}+\hat{\xi}_{23}^{D\,2}) \\
&\quad + 2U_{44}B_4^{B_s}b_4\hat{\xi}_{23}^{D}\hat{\xi}_{32}^{D\star}\Big) + \frac{1}{m_H^2}U_{44}B_4^{B_s}b_4\hat{\xi}_{23}^{D}\hat{\xi}_{32}^{D\star}\Bigg\},
\end{aligned} \tag{4.17}$$

JHEP02(2020)147

where we have defined $A_B \equiv f_{B_s}^2\, M_{B_s}^3/(4\,(m_b+m_s)^2) \simeq 0.105\,\text{GeV}^3$, and U_{ij} are elements of the evolution matrix in appendix C.

Figure 5 shows scatter plots of ΔM_{B_s}, including the 2HDM contribution both at tree and loop-level, versus $|\hat{\xi}_D^{32}|$ for different values of $\hat{\xi}_D^{23}$, $s_{\beta-\alpha}$, m_H and m_A. In the top plots, we fix $m_H = m_A = 200\,\text{GeV}$ and $\hat{\xi}_{23}^D = (\pm 1 \pm i) \times 10^{-4}$. Under this setup we can fit the experimental observation for the intervals $|\hat{\xi}_{32}^D| \sim [2\times 10^{-4}, 5\times 10^{-3}]$ for both $s_{\beta-\alpha} = 0.9$ (left plot) and $s_{\beta-\alpha} = 0.99$ (right plot). The total allowed interval is discontinuous and a second region as large as $|\hat{\xi}_{32}^D| \sim 3.5\times 10^{-2}$ is allowed for $s_{\beta-\alpha} = 0.99$. We can see that $|\hat{\xi}_{32}^D| \sim 3.6\times 10^{-2}$ is the largest Yukawa we expect for $s_{\beta-\alpha} \leq 0.99$. The bottom plots show $m_H = m_A = 2000\,\text{GeV}$ at a constant Yukawa of $\hat{\xi}_{23}^D = (\pm 1 \pm i)\times 10^{-3}$. For $s_{\beta-\alpha} = 0.99$ (right plot) we can attain a Yukawa as large as $|\hat{\xi}_{32}^D| \sim 1.6\times 10^{-2}$. We have also checked that in these regions the 2HDM is able to satisfy the observed value of the B_s^0–$\bar{B}_s^0$ mixing phase.

The 2HDM explanation of the discrepancy in terms of the tree-level contribution, also implies a prediction of $\text{BR}(h \to bs)$. For degenerate H, A, and much heavier than the light Higgs, the latter contribution to meson mixing dominates in eq. (4.17). This is true unless $c_{\beta-\alpha} \simeq 0$, for which in any case there is no contribution to $\text{BR}(h \to bs)$. Assuming a hierarchy in the off-diagonal Yukawas (taken real), for example $\hat{\xi}_{32}^D \gg \hat{\xi}_{23}^D$, so that the C_2 contribution to $\Delta M_{B_s,\,\text{2HDM}}$ dominates (and the mixed C_4 contribution can be neglected) we get from eqs. (3.19) and (4.17)

$$\text{BR}(h \to bs) \simeq \frac{3 m_h^3 m_H^2}{16\pi \Gamma_h (m_H^2 - m_h^2)}\, \frac{|\Delta M_{B_s,\,\text{2HDM}}|}{A_B\, |U_{22} B_2^{B_s}\, b_2 + U_{32} B_3^{B_s}\, b_3|} \simeq 2.1\times 10^{-4}\,, \tag{4.18}$$

where we used $\Delta M_{B_s,\,\text{2HDM}} = \Delta M_{B_s,\,\text{obs}} - \Delta M_{B_s,\,\text{SM}}$, and $\Gamma_h \simeq 4.07\cdot 10^{-3}\,\text{GeV}$. The prediction is identical if the other Yukawa dominates, $\hat{\xi}_{32}^D \ll \hat{\xi}_{23}^D$, so that C_2' dominates. On the other hand, for equal Yukawas $\hat{\xi}_{32}^D = \hat{\xi}_{23}^D$, the mixed C_4 contribution cannot be neglected, and there is an extra term proportional to $U_{44} B_4^{B_s} b_4$ inside the denominator of eq. (4.18), so that $\text{BR}(h \to bs) \simeq 6.3\times 10^{-5}$. As the angle $\beta - \alpha$ approaches $\pi/2$ this lower limit grows. We confirm these predictions with the scatter plots shown in figure 6, where we only have the SM plus the 2HDM tree-level contributions. We therefore conclude, that, if the observed discrepancy is confirmed, if accommodated in a 2HDM with negligible contributions at loop-level, it implies a prediction of $\text{BR}(h \to bs) \simeq 10^{-5}$–$10^{-4}$. In our numerical scan, we indeed can accommodate somewhat lower values, when new contributions from the heavy Higgses, and/or those beyond-tree-level containing the other Yukawas, are significant. Similar studies have been done in the context of SU(5) with two Higgs doublets [88].

4.3 Radiative decays: $\text{BR}(B \to X_s\gamma)$

In addition to B_s^0–$\bar{B}_s^0$ mixing, we are also interested in the constraints imposed by the radiative decay $B \to X_s\gamma$, that is the transition $b \to s\gamma$ at the quark level. NNLO predictions (i.e. next-to-next-to-leading order in QCD) can be found in refs. [89, 90]. In the context of the 2HDM, NNLO results can be found in ref. [91]; earlier NLO predictions [92, 93] are sufficient for the scope of the present work.

JHEP02(2020)147

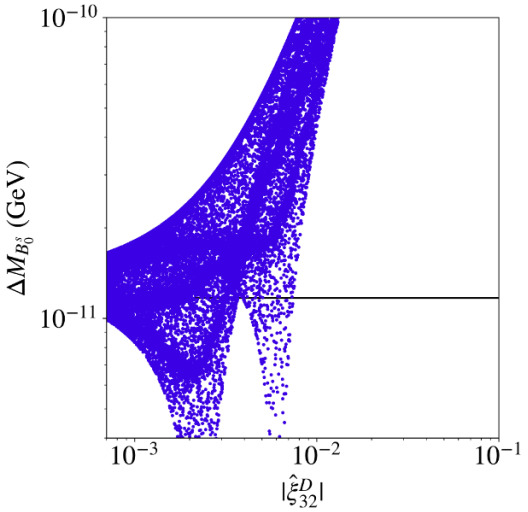

(a) $s_{\beta-\alpha} = 0.9$, $m_H = m_A = 200\,\text{GeV}$, $\hat{\xi}^D_{23} = (\pm 1 \pm i) \times 10^{-4}$.

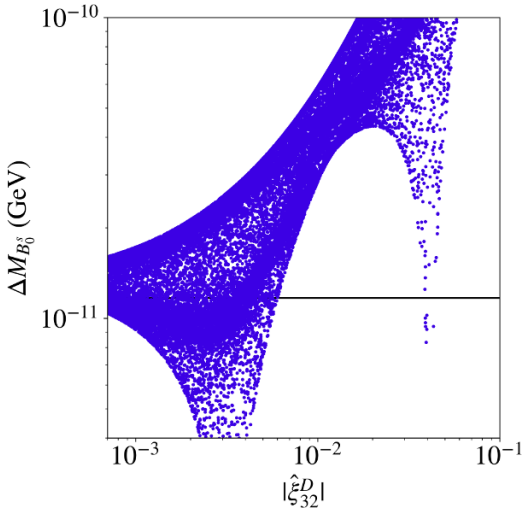

(b) $s_{\beta-\alpha} = 0.99$, $m_H = m_A = 200\,\text{GeV}$, $\hat{\xi}^D_{23} = (\pm 1 \pm i) \times 10^{-4}$.

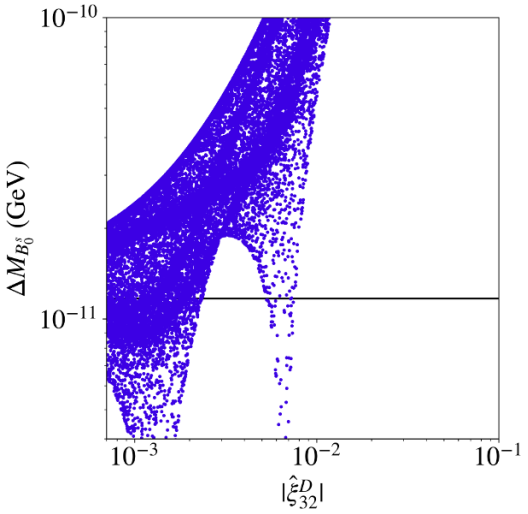

(c) $s_{\beta-\alpha} = 0.9$, $m_H = m_A = 2000\,\text{GeV}$, $\hat{\xi}^D_{23} = (\pm 1 \pm i) \times 10^{-3}$.

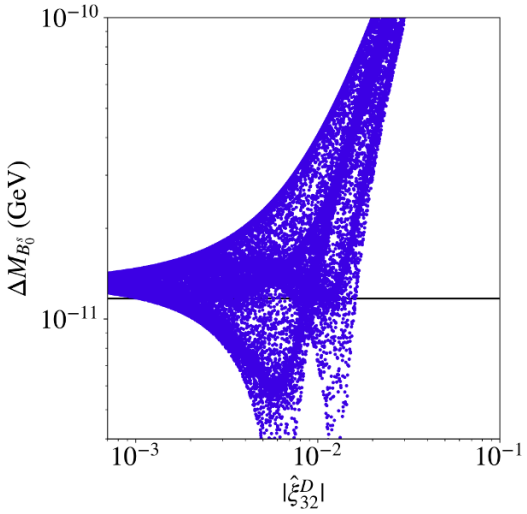

(d) $s_{\beta-\alpha} = 0.99$, $m_H = m_A = 2000\,\text{GeV}$, $\hat{\xi}^D_{23} = (\pm 1 \pm i) \times 10^{-3}$.

Figure 5. ΔM_{B_s} in the 2HDM versus $|\hat{\xi}^D_{32}|$. The horizontal line shows the observed value (the corresponding error is smaller than the width of the line itself). The different values of $s_{\beta-\alpha}$, m_H, m_A and $\hat{\xi}^D_{23}$ used in the analyses are shown in each case.

The basis of operators that describes this $|\Delta B| = 1$ process includes four quark current-current ($O_{1,2}$) and penguin (O_{3-6}) operators, together with photonic (O_7) and gluonic (O_8) dipole operators (see, e.g., ref. [94]). Effective Wilson coefficients $C_{7,8[\text{eff}]}$ are usually defined such that the perturbative contribution to $\text{BR}(B \to X_s\gamma)$ is proportional to $|C_{7[\text{eff}]}|^2$ at leading order. Expressions for the LO and NLO contributions to the Wilson coefficients (at the matching scale $\mu_W \sim m_W$) can be found in eqs. (16) and (17) of ref. [93]. Leading order contributions involving neutral scalars can be found in ref. [29].[5] The perturbative

[5]For comparison with the notation of ref. [93], $(XY^*)^{\phi}_{u_i} = -1/(m_{u_i} m_b)\, \Gamma^{LR\,\phi *}_{u_i\, d_3} \Gamma^{RL\,\phi}_{u_i\, d_2}$ and $(YY^*)^{\phi}_{u_i} = 1/(m^2_{u_i})\, \Gamma^{RL\,\phi *}_{u_i\, d_3} \Gamma^{RL\,\phi}_{u_i\, d_2}$.

JHEP02(2020)147

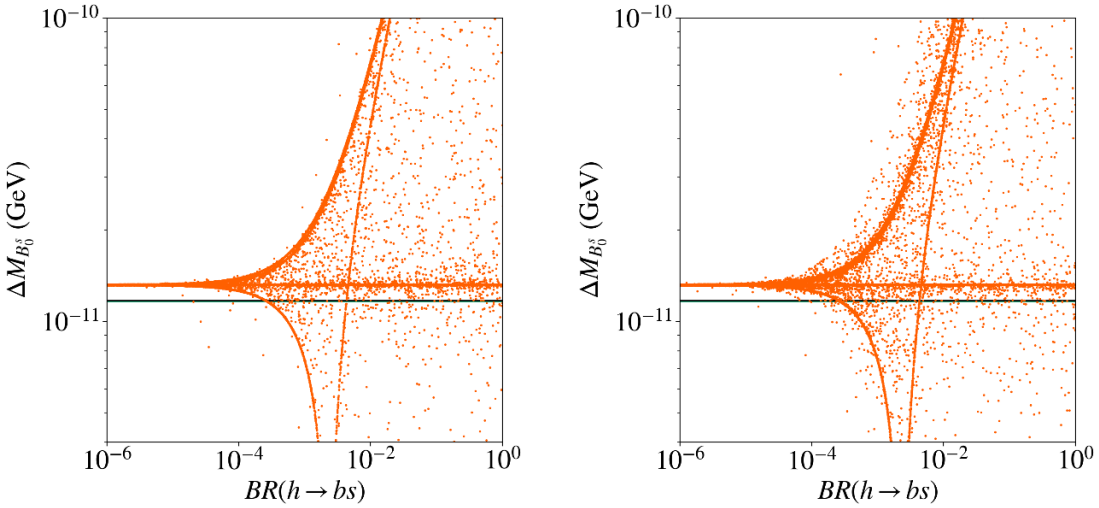

(a) $\hat{\xi}^D_{23} \gg \hat{\xi}^D_{32}$, or $\hat{\xi}^D_{23} \ll \hat{\xi}^D_{32}$. **(b)** $\hat{\xi}^D_{23} = \hat{\xi}^D_{32}$.

Figure 6. Mass splitting ΔM_{B_s}, stemming from the SM and the 2HDM at tree-level, versus $\mathrm{BR}(h \to bs)$. We set $m_H = m_A = 2000\,\mathrm{GeV}$ and $s_{\beta-\alpha} = 0.9$. The horizontal line shows the observed value (the corresponding error is smaller than the width of the line itself). We see lower values of $\mathrm{BR}(h \to bs)$ being more accessible for the case $\hat{\xi}^D_{23} = \hat{\xi}^D_{32}$.

$b \to s\gamma$ decay rate is given by

$$\Gamma(b \to s\gamma) = \frac{G_F^2}{32\pi^4} |V_{ts}^* V_{tb}|^2 \alpha_{\mathrm{em}}\, m_b^5 \left(|C_{7\mathrm{eff}}(\mu_b)|^2 + |C'_{7\mathrm{eff}}(\mu_b)|^2 \right). \tag{4.19}$$

The inclusive $\bar{B} \to X_s\gamma$ decay rate is measured with photon energies $E_\gamma > 1.6\,\mathrm{GeV}$, in which case the non-perturbative contributions relating the quark level and the meson decay rates are below the 5% level [95]. Attending to the different sources of theoretical uncertainty, in order to place constraints on the 2HDM contributions, we use the perturbative quark level decay rate in eq. (4.19) with a conservative theoretical error of 10%. The corresponding SM calculation is given in table 5 and is in very good agreement with the observed value.

5 Numerical analysis

5.1 Parameter scan

Given the large number of parameters of our general 2HDM (9 from the potential, 12 from the Yukawas in the 2–3 plane) we use a global fit using MultiNest [96] to scan over the allowed parameter space. We also use 2HDMC (Two-Higgs-Doublet Model Calculator) [61] to perform some phenomenological calculations. We do not include the SM one loop contribution to $h \to bs$ or $t \to ch$, but we compute the new 2HDM contributions. We then plot our results using pippi [97]. The parameters and priors scanned over are given in table 6. We use the Higgs basis. To ensure that we carry out our scan over both quadrants in the physical angle we choose $-\pi/2 \leq (\beta - \alpha) \leq \pi/2$.

JHEP02(2020)147

Parameter	Range	Prior
$\Lambda_{1,2,3,4,5,7}$	$\pm[10^{-15}, 4\pi]$	Log
$\beta - \alpha$	$[-\pi/2, \pi/2]$	Flat
M_{22}^2 (GeV^2)	$[10^4, 10^7]$	Flat
$\mathrm{Re}(\hat{\xi}_{ij}^{D,U})$	$\pm[10^{-15}, 4\pi]$	Log
$\mathrm{Im}(\hat{\xi}_{ij}^{D,U})$	$\pm[10^{-15}, 4\pi]$	Log

Table 6. Parameters scanned over. We also indicate whether the priors are flat or log. In the Yukawa sector, $i, j = 2, 3$, and all other couplings are zero.

We need to provide likelihood functions $\mathcal{L}$ (or $\chi^2 = -2\ln\mathcal{L}$) to scan the parameter space of the model. To ensure that the masses of the scalars are positive, as well as to impose stability of the scalar potential, we use a hard cut-off: for a calculated value $\mathcal{O}_{\rm calc}$ and lower bound B_i

$$\chi^2_{\rm bounds} = \begin{cases} 0, & \text{if } \mathcal{O}_{\rm calc} > B_i \\ \chi_{\rm max}, & \text{if } \mathcal{O}_{\rm calc} \leq B_i, \end{cases} \tag{5.1}$$

where $\chi_{\rm max}$ is large enough that the scanner effectively invalidates the point. The reverse of this may be used for an upper bound. Unitarity and perturbativity are imposed by a soft cut-off

$$\chi^2_{\rm bounds} = \begin{cases} 0, & \text{if } \mathcal{O}_{\rm calc} < B_i/0.64 \\ \left(\frac{0.64\mathcal{O}_{\rm calc}}{B_i} - 1\right)^2, & \text{if } \mathcal{O}_{\rm calc} \geq B_i/0.64\,, \end{cases} \tag{5.2}$$

where B_i is the upper bound at 68% confidence (improving the guidance provided to the scanner). For observables that have been measured we use a centered distribution with the observed value at $\mathcal{O}_{\rm obs}$ and error σ

$$\chi^2_{\rm observations} = \left(\frac{\mathcal{O}_{\rm calc} - \mathcal{O}_{\rm obs}}{\sigma}\right)^2. \tag{5.3}$$

The final χ^2-like function is built from all M bounds and N observations,

$$\chi^2 = \sum_i^M \chi^2_{{\rm bounds},i} + \sum_i^N \chi^2_{{\rm observations},i}\,. \tag{5.4}$$

For B_s^0–$\bar{B}_s^0$ mixing and $B \to X_s\gamma$, we sum the errors of experimental and calculated values in quadrature.

5.2 Results

To start with, we show in figure 7 the experimental contributions to the total χ^2 value that we calculate in the SM limit, that is $s_{\beta-\alpha} \to 1$ and $\hat{\xi}_{ij}^U = \hat{\xi}_{ij}^D = 0$. The largest pulls

JHEP02(2020)147

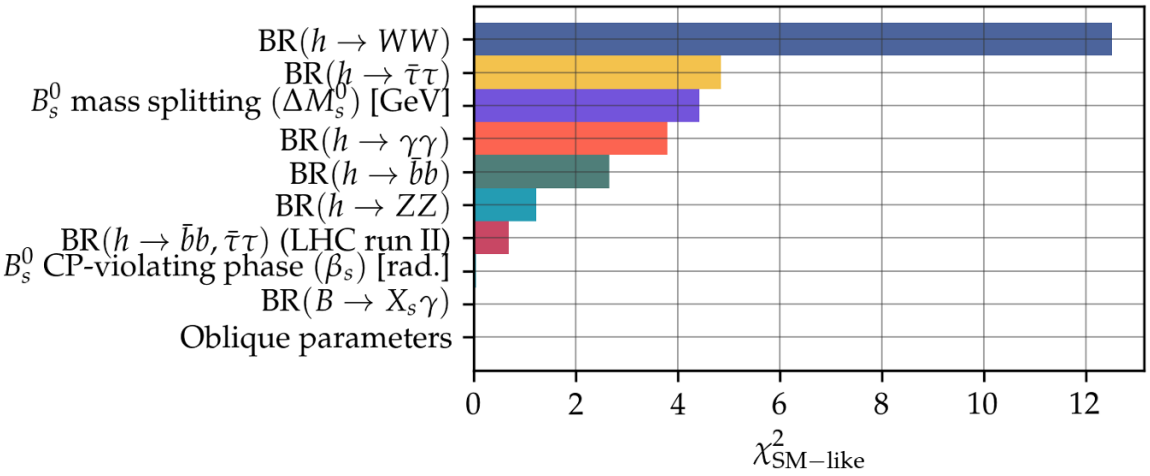

Figure 7. χ^2 contributions due to experimental constraints in the limit of the Standard Model, $s_{\beta-\alpha} \to 1$ and $\hat{\xi}^U_{ij} = \hat{\xi}^D_{ij} = 0$.

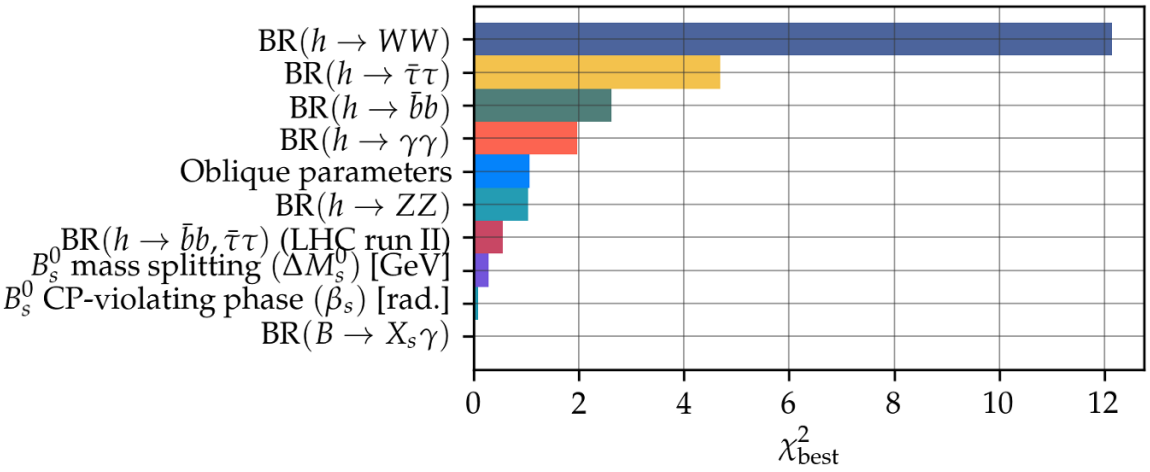

Figure 8. The contributions from each of the constraints to the best-fit χ^2 in our global scan of the 2HDM.

here come from SM Higgs decays, as expected predominantly from $h \to WW$, due to the fact that the experimental values of some of the production channels are slightly off from the SM, see eq. (3.27). LHC Run II data [98–100] gives the $h \to WW$ signal strengths by production channel (as in eq. (3.27)) as $(1.10^{+0.21}_{-0.21}, 0.62^{+0.36}_{-0.35}, 2.3^{+1.2}_{-1.0}, 2.9^{+1.9}_{-1.3}, 1.5^{+0.6}_{-0.6})$. This almost halves the $h \to WW$ channel $\chi^2_{\text{SM-limit}}$ contribution to ~ 7. As such, had we included LHC Run II data in our fit we would improve our χ^2 from this degree of freedom. In any case, the SM is consistent with this data at the $\sim 2\sigma$ level.

In figure 8 we show the pull from each constraint at our best fit point for the 2HDM. This occurs at heavy scalar masses ($m_H = m_A = m_{H^\pm}$) of 2450 GeV. Relative to the $\chi^2_{\text{SM-limit}}$ shown in figure 7, we see that the Higgs decay channels are very similar, except for the decrease in the $h \to \gamma\gamma$ channel. There is a small pull from the oblique parameters. In light of the combined fit, the pull for oblique parameters is optimised at heavier masses,

JHEP02(2020)147

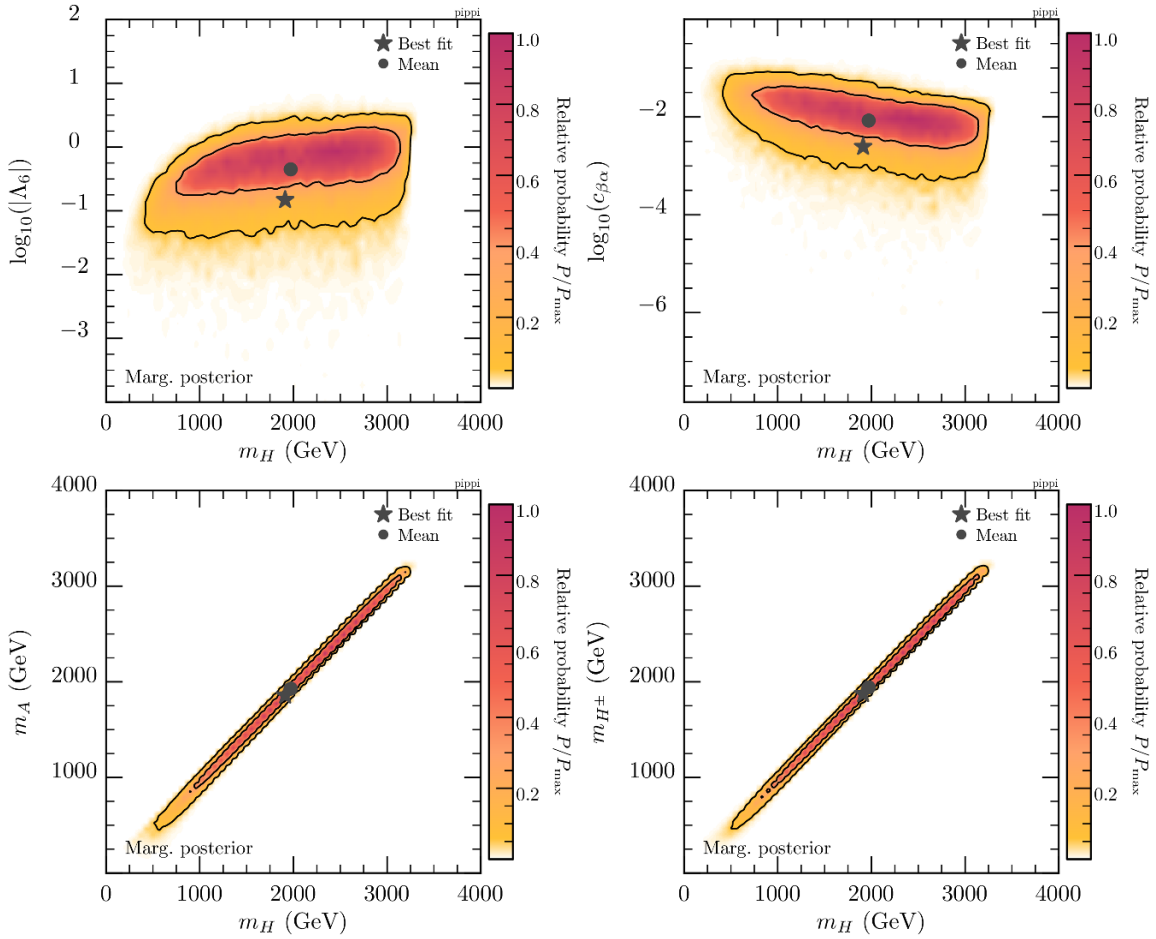

Figure 9. *Top left [right]*: $\log_{10}(|\Lambda_6|)$ [$\log_{10}(c_{\beta-\alpha})$] versus m_H. *Bottom left [right]*: relationships between the extra scalar particles of the 2HDM, m_A [$m_H^\pm$] versus m_H. The 1σ and 2σ probability regions are represented by the solid lines.

$\sim 3\,\text{TeV}$, where it falls to $\chi^2 = 0.4$. Notably, flavor observables are well minimised at the best-fit point. Especially the B_s^0 meson mixing discrepancy present in the SM (as discussed in section 4.2.3) is reduced in the 2HDM.

In the top panels of figure 9, we plot $\log_{10}(|\Lambda_6|)$ (left) and $\log_{10}(c_{\beta-\alpha})$ (right) versus m_H. On the top-left there is a correlation between Λ_6 and m_H (as expected from eq. (3.10) for a sufficiently SM-like Higgs boson, i.e., in the alignment limit $s_{\beta-\alpha} \to 1$). The bottom panels display correlations between the extra scalars. They each obey a linear relationship imposed by the oblique parameter constraints. The size of our masses extends up to $\sim 3200\,\text{GeV}$ due to the priors on M_{22} and the perturbativity limits used on the quartic couplings.

In figure 10 we plot the logarithm of the absolute value of the off-diagonal Yukawa combinations ($\log_{10}(|\hat{\xi}^D_{23}|)$ and $\log_{10}(|\hat{\xi}^D_{32}|)$) versus $\log_{10}[\text{BR}(h \to bs)]$. We attain an upper (lower) limit on $\text{BR}(h \to bs)$ of $\sim 10^{-3}$ ($\sim 10^{-12}$) at 1σ.

Exploring the constraints that caused these limits, we show in figure 11 the posterior distributions of relevant flavor physics observables (the mass splitting ΔM_{B_s}, the CP vio-

JHEP02(2020)147

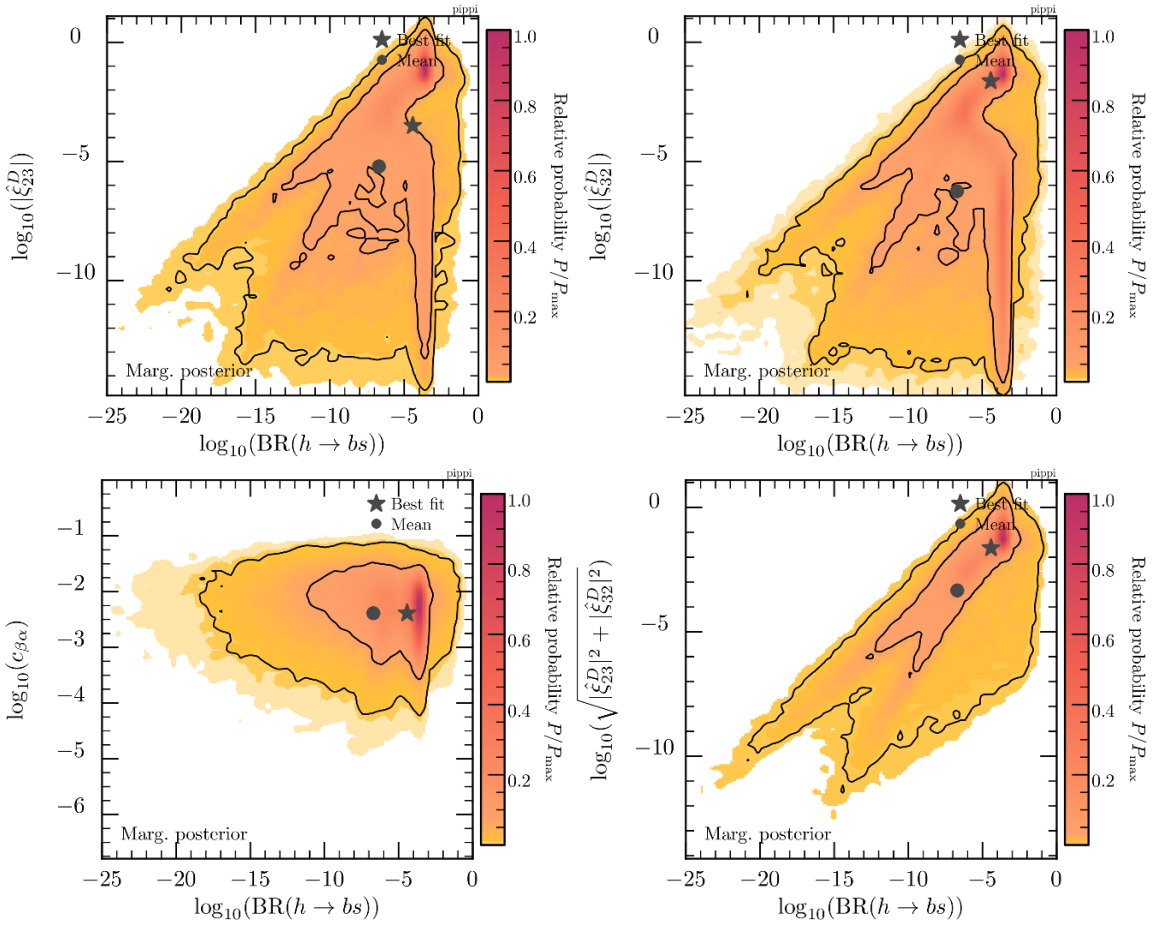

Figure 10. Off-diagonal down-quark Yukawa couplings $\hat{\xi}^D$ versus $\log_{10}[\mathrm{BR}(h \to bs)]$. *Top left [right]*: $\log_{10}(|\hat{\xi}^D_{23}|)$ $[\log_{10}(|\hat{\xi}^D_{32}|)]$ *Bottom left*: the logarithm of the physical angle $c_{\beta-\alpha}$ versus $\log_{10}[\mathrm{BR}(h \to bs)]$. *Bottom right*: logarithm of the modulus of the off-diagonal contributions to $\hat{\xi}^D$ versus $\log_{10}[\mathrm{BR}(h \to bs)]$.

lating phase β_s and the radiative B-decay, $B \to X_s\gamma$) with respect to the $h \to bs$ decay. For ΔM_{B_s} we observe two solution regions, as expected from figure 5. In the upper region, the predicted ΔM_{B_s} mass splitting coincides with the SM value, which is 1.8σ away from the observed value. In the lower region, the 2HDM can accommodate the observed value, and what is more interesting, this yields a lower bound $\mathrm{BR}(h \to bs)$, at the level of 10^{-5}–10^{-4} (at 1σ). This lower bound coincides well with our tree-level prediction (4.18).

In figure 12 we plot the B^0_s meson mixing mass splitting and $B \to X_s\gamma$ versus $\mathrm{BR}(t \to ch)$. For radiative B-decays, the combinations $\xi^U_{23}\,\xi^U_{33}\,m_t$ with tops and $\xi^U_{23}\,\xi^D_{33}\,m_b$ with bottoms in the loop, enter. On the other hand, Higgs data favours somewhat large diagonal Yukawa contributions. This in turn implies some (weak) upper bounds on ξ^U_{23}. The upper limit on the $\mathrm{BR}(t \to ch)$ comes from the LHC observed upper limit, 2.2×10^{-3} (see eq. (1.1)), hence, indirect constraints are weaker. As such, there is still almost an order of magnitude of precision before we may begin exploring the allowed 2HDM region at colliders. In this case, no lower bounds have been found from our scans, these are again just from the priors.

JHEP02(2020)147

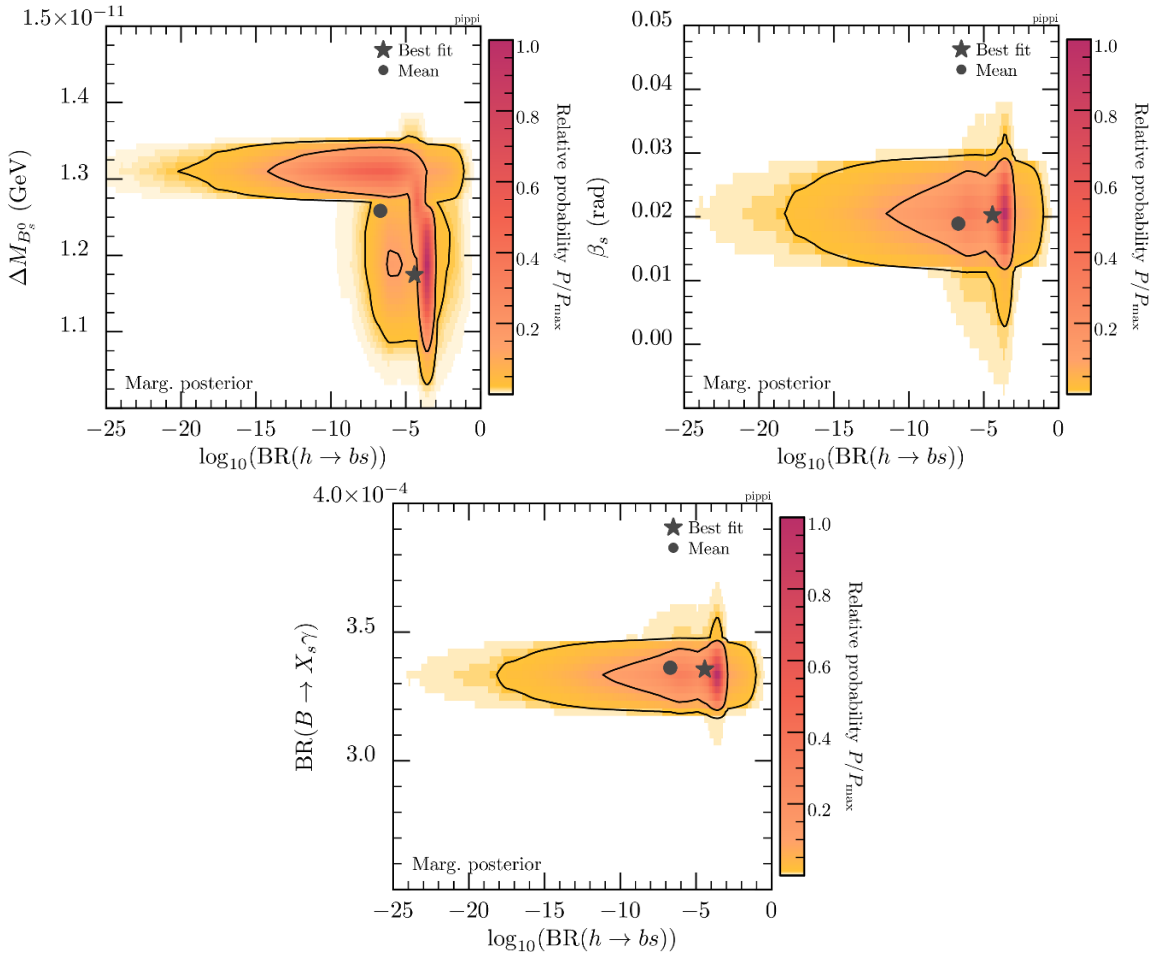

Figure 11. Different observables and parameter versus $\log_{10}[\mathrm{BR}(h \to bs)]$. *Top left [right]*: B_s^0 meson mixing mass splitting [CP phase]. *Bottom*: Radiative B decay $\mathrm{BR}(B \to X_s\gamma)$.

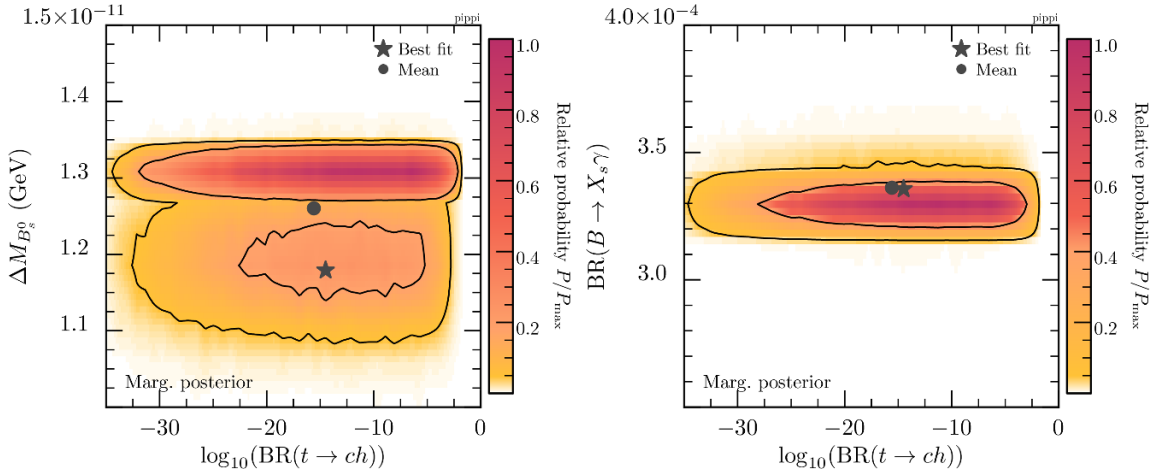

Figure 12. Different observables and parameters versus $\log_{10}[\mathrm{BR}(t \to ch)]$. *Left*: B_s^0 meson mixing mass splitting. *Right*: radiative B decays.

JHEP02(2020)147

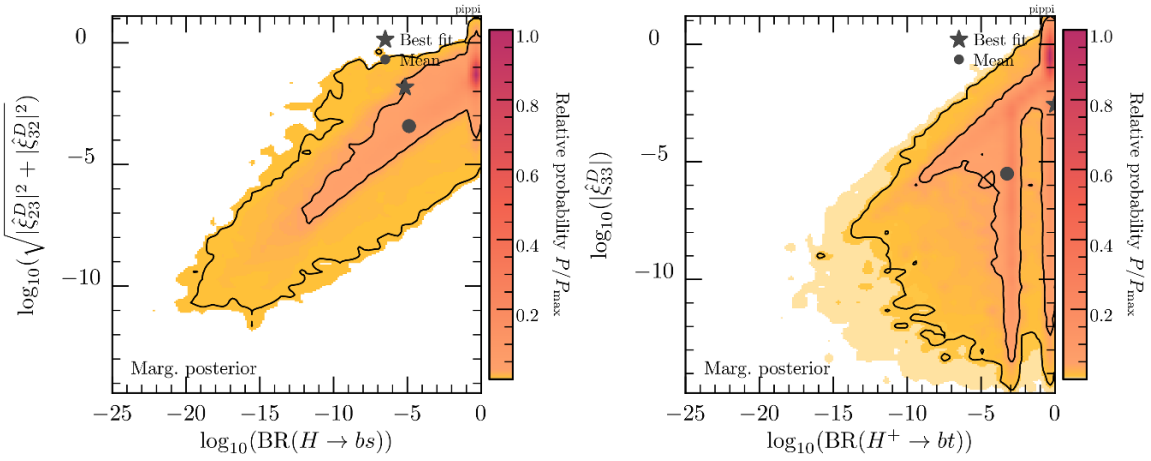

Figure 13. *Left*: $\log_{10}(|\hat{\xi}^D_{23}|^2 + |\hat{\xi}^D_{32}|^2)^{1/2}$ versus $\log(\mathrm{BR}(H \to bs))$. *Right*: $\log_{10}(|\hat{\xi}^D_{33}|)$ versus $\log(\mathrm{BR}(H^+ \to tb))$.

It is also interesting to investigate flavor violation in the new scalar sector, that is decays involving H, A and $H^\pm$. Figure 13 displays the modulus of the relevant off-diagonal Yukawas versus $\mathrm{BR}(H \to bs)$. Similar plots are obtained for $A \to bs$, tc, and $H \to tc$. It is remarkable that these flavor-changing decays can saturate the decay widths of the heavy scalars. This may be relevant for direct searches. We also note that $H^+ \to tb$ has the largest lower bound.

6 Conclusions

In this work, we have investigated quark flavor violation involving the second and third families from an effective field theory point of view. We concentrated on the interesting processes $h \to bs$ and $t \to ch$. After outlining the possible tree-level simplified models, which involve new scalars and/or vector-like quarks, and estimating their contributions to HQFV processes, we have focused on the most promising scenario to produce large signals: a general (or Type III) 2HDM.

We carried out a comprehensive global scan of the 2HDM imposing theoretical and experimental constraints. We focused primarily on B-physics constraints coming from B^0_s meson mixing (mass splitting and CP violating phase) and the radiative decay $B \to X_s\gamma$, which impose the most significant restrictions on the non-diagonal Yukawa elements $\hat{\xi}^D_{23,32}$ and $\hat{\xi}^U_{23,32}$. We have also obtained that the $\sim 2\sigma$ mass-splitting discrepancy with respect to the SM in the B_s meson system can be accommodated in the 2HDM at tree-level, yielding a lower bound prediction of $\mathrm{BR}(h \to bs) \simeq 10^{-5}$–$10^{-4}$ if loop-level and heavy Higgs contributions are not significant.

The final values obtained in our full parameter scan are $\mathrm{BR}(h \to bs) < 10^{-3}\,(10^{-1})$ and $\mathrm{BR}(t \to ch) < 6 \times 10^{-4}\,(10^{-2})$ at 1 and 2σ (lower bounds, if present, are at the level of the one-loop SM prediction). This parameter space is already accessible and can be further examined at future colliders [101]. For example, a future 100 TeV proton-proton collider is able to constrain the $t \to ch$ channel at $O(10^{-5})$ [102]. Beyond the two hallmark decays,

JHEP02(2020)147

possibly the easiest HQFV process to observe is $H^+ \to tb$ due to its large production cross section and the possible large branching fraction.

Any observed (therefore sizeable) signal of quark flavor violation involving the Higgs boson would clearly point to physics beyond the SM. As we have studied in this work, the stringent limits from low energy observables imply that it would most possibly stem from a 2HDM. We have demonstrated that the allowed parameter space in the up and the down sectors allowed by current upper limits are well within reach.

Acknowledgments

We are grateful to A. Azatov for useful discussions. This work has been supported in part by the Australian Research Council through the Centre of Excellence for Particle Physics at the Terascale CE110001004. MN acknowledges support from Fundação para a Ciência e a Tecnologia (FCT, Portugal) through the projects UID/FIS/00777/2019, CERN/FIS-PAR/0004/2017, and PTDC/FIS-PAR/29436/2017. JHG acknowledges financial support from the H2020-MSCA-RISE project "InvisiblesPlus", and he thanks the Theoretical Physics Department of Fermilab, where this project was completed, for the kind hospitality. MW is supported by the Australian Research Council Future Fellowship FT140100244.

A Derivative operators for vector-like quarks

In table 7 we list the quantum numbers $(2T+1, T_3, Y)$ of the different SM (EFT) quark objects on which the covariant derivative acts in order to derive the Z, W couplings. Details on the procedure are given in ref. [30]. In *Diff.* we just take the difference of the pair $(T_3, Y)_{\rm EFT} - (T_3, Y)_{\rm SM}$ which will give us the "left-over" combination of W_3 and B fields, and therefore the Z and W interactions.

B Parameter values

The SM values used for the calculation are presented in table 8 and relevant parameters for meson mixing are given in table 9. The complex CKM matrix we use in our calculation is attained from UTFit 2016 SM Fits [103], and reads

$$V = \begin{pmatrix} 0.97431 & 0.22512 & 0.00365e^{-65.88i} \\ -0.22497e^{0.0352i} & 0.97344e^{-0.001877i} & 0.04255 \\ 0.00869e^{-22.0i} & -0.04156e^{1.040i} & 0.999097 \end{pmatrix} . \tag{B.1}$$

C Evolution matrix for meson mixing

We extract the RGE matrix for the Meson Mixing basis introduced in eq. (4.6) using DSixTools [82]. This matrix represents the running of the operators from $\mu_i = m_W$ to

JHEP02(2020)147

	Part	SM	EFT	Diff.	$d_R Z$	$d_L Z$	$u_R Z$	$u_L Z$	W
$d_R\Phi$	d_R	$(1,0,-1/3)$	$\left(2,-\frac{1}{2},\frac{1}{6}\right)$	$-\left(\frac{1}{2},-\frac{1}{2}\right)$	-1				
$d_R\tilde{\Phi}$	d_R	$(1,0,-1/3)$	$\left(2,\frac{1}{2},-\frac{5}{6}\right)$	$\left(\frac{1}{2},-\frac{1}{2}\right)$	$+1$				
$u_R\Phi$	u_R	$(1,0,2/3)$	$\left(2,-\frac{1}{2},\frac{7}{6}\right)$	$-\left(\frac{1}{2},-\frac{1}{2}\right)$			-1		
$u_R\tilde{\Phi}$	u_R	$(1,0,2/3)$	$\left(2,\frac{1}{2},\frac{1}{6}\right)$	$\left(\frac{1}{2},-\frac{1}{2}\right)$			$+1$		
$\Phi^\dagger Q$	d_L	$\left(2,-\frac{1}{2},\frac{1}{6}\right)$	$(1,0,-1/3)$	$\left(\frac{1}{2},-\frac{1}{2}\right)$		$+1$			-1
$\tilde{\Phi}^\dagger Q$	u_L	$\left(2,\frac{1}{2},\frac{1}{6}\right)$	$(1,0,2/3)$	$-\left(\frac{1}{2},-\frac{1}{2}\right)$				-1	-1
$\Phi^\dagger\vec{\tau}Q$	$-d_L$	$\left(2,-\frac{1}{2},\frac{1}{6}\right)$	$(3,0,-1/3)$	$\left(\frac{1}{2},-\frac{1}{2}\right)$		$+1$			
	$\sqrt{2}u_L$	$\left(2,\frac{1}{2},\frac{1}{6}\right)$	$(3,1,-1/3)$	$\left(\frac{1}{2},-\frac{1}{2}\right)$				$+2$	
$\tilde{\Phi}^\dagger\vec{\tau}Q$	$\sqrt{2}d_L$	$\left(2,-\frac{1}{2},\frac{1}{6}\right)$	$(3,-1,2/3)$	$-\left(\frac{1}{2},-\frac{1}{2}\right)$		-2			
	u_L	$\left(2,\frac{1}{2},\frac{1}{6}\right)$	$(3,0,2/3)$	$-\left(\frac{1}{2},-\frac{1}{2}\right)$				-1	

Table 7. Derivation of FCNC interactions generated by *Derivative operators*. Z couplings are in units of $y_q v/m_q \times e/(2c_W s_W)$, while W ones are in units of $V y_q v/m_q \times e/(2\sqrt{2}s_W)$.

Parameter	Value	Parameter	Value
m_u	2.2×10^{-3} GeV	$\alpha_{\rm em}(m_Z)$	1/127.934
m_c	1.67 GeV	α^0	1/137.036
$\overline{m_c}(m_c)$	1.273 GeV [104]	$G_{\rm F}$	1.16638×10^{-5} GeV^{-2}
m_t	173.5 GeV	$\alpha_s(m_Z)$	0.1182
$\overline{m_t}(m_t)$	(173.5−10.38) GeV [105]	m_W	80.385 GeV
m_d	4.7×10^{-3} GeV	m_Z	91.1876 GeV
m_s	0.096 GeV		
m_b	4.78 GeV		
$\overline{m_b}(m_b)$	4.197 GeV [104]		

Table 8. Standard Model values used for global scan, attained from ref. [16] where not explicitly stated otherwise. Parameters dependant on scale are normalised in the $\overline{\rm MS}$ scheme while non scheme dependant masses are assumed to be given as pole masses.

JHEP02(2020)147

Meson Mass [16]		Decay Constant [16]		Bag factors [106]	
M_{B_s}	5.36689 GeV	f_{B_s}	0.224 GeV	$B_1^{B_s}(\mu_b)$	0.87
				$B_2^{B_s}(\mu_b)$	0.80
				$B_3^{B_s}(\mu_b)$	0.93
				$B_4^{B_s}(\mu_b)$	1.16
				$B_5^{B_s}(\mu_b)$	1.75

Table 9. Values of $B_i(\mu)$ are renormalised in the $\overline{\text{MS}}$ scheme. The B-meson decay constant and mass are also provided.

$\mu_f = m_B$:

$$U(m_B, m_W) = \begin{pmatrix} 0.862096 & 0 & 0 & 0 & 0 & 0 & 0 & 0 \\ 0 & 1.41304 & -0.197994 & 0 & 0 & 0 & 0 & 0 \\ 0 & -0.0516513 & 0.682309 & 0 & 0 & 0 & 0 & 0 \\ 0 & 0 & 0 & 1.79804 & 0.288788 & 0 & 0 & 0 \\ 0 & 0 & 0 & 0 & 0.931673 & 0 & 0 & 0 \\ 0 & 0 & 0 & 0 & 0 & 0.862096 & 0 & 0 \\ 0 & 0 & 0 & 0 & 0 & 0 & 1.41304 & -0.197994 \\ 0 & 0 & 0 & 0 & 0 & 0 & -0.0516513 & 0.682309 \end{pmatrix} \tag{C.1}$$

References

[1] ATLAS collaboration, *Observation of a new particle in the search for the Standard Model Higgs boson with the ATLAS detector at the LHC*, *Phys. Lett.* **B 716** (2012) 1 [arXiv:1207.7214] [INSPIRE].

[2] CMS collaboration, *Observation of a New Boson at a Mass of 125 GeV with the CMS Experiment at the LHC*, *Phys. Lett.* **B 716** (2012) 30 [arXiv:1207.7235] [INSPIRE].

[3] J.A. Aguilar-Saavedra, *Top flavor-changing neutral interactions: Theoretical expectations and experimental detection*, *Acta Phys. Polon.* **B 35** (2004) 2695 [hep-ph/0409342] [INSPIRE].

[4] J.M. Yang, *Probing new physics from top quark FCNC processes at linear colliders: A Mini review*, *Annals Phys.* **316** (2005) 529 [hep-ph/0409351] [INSPIRE].

[5] F. Larios, R. Martinez and M.A. Perez, *New physics effects in the flavor-changing neutral couplings of the top quark*, *Int. J. Mod. Phys.* **A 21** (2006) 3473 [hep-ph/0605003] [INSPIRE].

JHEP02(2020)147

[6] P.M. Ferreira, R.B. Guedes and R. Santos, *Combined effects of strong and electroweak FCNC effective operators in top quark physics at the CERN LHC*, *Phys. Rev.* **D 77** (2008) 114008 [arXiv:0802.2075] [INSPIRE].

[7] N. Craig et al., *Searching for $t \to ch$ with Multi-Leptons*, *Phys. Rev.* **D 86** (2012) 075002 [arXiv:1207.6794] [INSPIRE].

[8] R. Harnik, J. Kopp and J. Zupan, *Flavor Violating Higgs Decays*, *JHEP* **03** (2013) 026 [arXiv:1209.1397] [INSPIRE].

[9] C. Degrande, F. Maltoni, J. Wang and C. Zhang, *Automatic computations at next-to-leading order in QCD for top-quark flavor-changing neutral processes*, *Phys. Rev.* **D 91** (2015) 034024 [arXiv:1412.5594] [INSPIRE].

[10] G. Abbas, A. Celis, X.-Q. Li, J. Lu and A. Pich, *Flavour-changing top decays in the aligned two-Higgs-doublet model*, *JHEP* **06** (2015) 005 [arXiv:1503.06423] [INSPIRE].

[11] B. Altunkaynak, W.-S. Hou, C. Kao, M. Kohda and B. McCoy, *Flavor Changing Heavy Higgs Interactions at the LHC*, *Phys. Lett.* **B 751** (2015) 135 [arXiv:1506.00651] [INSPIRE].

[12] V. Cirigliano, W. Dekens, J. de Vries and E. Mereghetti, *Constraining the top-Higgs sector of the Standard Model Effective Field Theory*, *Phys. Rev.* **D 94** (2016) 034031 [arXiv:1605.04311] [INSPIRE].

[13] W. Altmannshofer and B. Maddock, *Flavorful Two Higgs Doublet Models with a Twist*, *Phys. Rev.* **D 98** (2018) 075005 [arXiv:1805.08659] [INSPIRE].

[14] W. Altmannshofer, B. Maddock and D. Tuckler, *Rare Top Decays as Probes of Flavorful Higgs Bosons*, *Phys. Rev.* **D 100** (2019) 015003 [arXiv:1904.10956] [INSPIRE].

[15] M. Badziak and K. Harigaya, *Asymptotically Free Natural Supersymmetric Twin Higgs Model*, *Phys. Rev. Lett.* **120** (2018) 211803 [arXiv:1711.11040] [INSPIRE].

[16] Particle Data Group, *Review of Particle Physics*, *Chin. Phys.* **C 40** (2016) 100001 [INSPIRE].

[17] ATLAS collaboration, *Search for top quark decays $t \to qH$, with $H \to \gamma\gamma$, in $\sqrt{s} = 13$ TeV pp collisions using the ATLAS detector*, *JHEP* **10** (2017) 129 [arXiv:1707.01404] [INSPIRE].

[18] CMS collaboration, *Search for the flavor-changing neutral current interactions of the top quark and the Higgs boson which decays into a pair of b quarks at $\sqrt{s} = 13$ TeV*, *JHEP* **06** (2018) 102 [arXiv:1712.02399] [INSPIRE].

[19] ATLAS collaboration, *Search for flavor-changing neutral currents in top quark decays $t \to Hc$ and $t \to Hu$ in multilepton final states in proton-proton collisions at $\sqrt{s} = 13$ TeV with the ATLAS detector*, *Phys. Rev.* **D 98** (2018) 032002 [arXiv:1805.03483] [INSPIRE].

[20] D0 collaboration, *Search for Flavor Changing Neutral Currents in Decays of Top Quarks*, *Phys. Lett.* **B 701** (2011) 313 [arXiv:1103.4574] [INSPIRE].

[21] CMS collaboration, *Search for Flavor-Changing Neutral Currents in Top-Quark Decays $t \to Zq$ in pp Collisions at $\sqrt{s} = 8$ TeV*, *Phys. Rev. Lett.* **112** (2014) 171802 [arXiv:1312.4194] [INSPIRE].

[22] CMS collaboration, *Search for associated production of a Z boson with a single top quark and for tZ flavour-changing interactions in pp collisions at $\sqrt{s} = 8$ TeV*, *JHEP* **07** (2017) 003 [arXiv:1702.01404] [INSPIRE].

JHEP02(2020)147

[23] ATLAS collaboration, *Search for flavour-changing neutral current top-quark decays to qZ in pp collision data collected with the ATLAS detector at* $\sqrt{s} = 8$ *TeV*, *Eur. Phys. J.* **C 76** (2016) 12 [arXiv:1508.05796] [INSPIRE].

[24] ATLAS collaboration, *Search for flavour-changing neutral current top-quark decays* $t \to qZ$ *in proton-proton collisions at* $\sqrt{s} = 13$ *TeV with the ATLAS detector*, *JHEP* **07** (2018) 176 [arXiv:1803.09923] [INSPIRE].

[25] ATLAS collaboration, *Search for single top-quark production via flavour-changing neutral currents at 8 TeV with the ATLAS detector*, *Eur. Phys. J.* **C 76** (2016) 55 [arXiv:1509.00294] [INSPIRE].

[26] CMS collaboration, *Search for Anomalous Single Top Quark Production in Association with a Photon in pp Collisions at* $\sqrt{s} = 8$ *TeV*, *JHEP* **04** (2016) 035 [arXiv:1511.03951] [INSPIRE].

[27] G. Blankenburg, J. Ellis and G. Isidori, *Flavour-Changing Decays of a 125 GeV Higgs-like Particle*, *Phys. Lett.* **B 712** (2012) 386 [arXiv:1202.5704] [INSPIRE].

[28] D. Barducci and A.J. Helmboldt, *Quark flavour-violating Higgs decays at the ILC*, *JHEP* **12** (2017) 105 [arXiv:1710.06657] [INSPIRE].

[29] A. Crivellin, J. Heeck and D. Müller, *Large* $h \to bs$ *in generic two-Higgs-doublet models*, *Phys. Rev.* **D 97** (2018) 035008 [arXiv:1710.04663] [INSPIRE].

[30] J. Herrero-Garcia, N. Rius and A. Santamaria, *Higgs lepton flavour violation: UV completions and connection to neutrino masses*, *JHEP* **11** (2016) 084 [arXiv:1605.06091] [INSPIRE].

[31] L.G. Benitez-Guzmán, I. García-Jiménez, M.A. López-Osorio, E. Martínez-Pascual and J.J. Toscano, *Revisiting the flavor changing neutral current Higgs decays* $H \to q_i q_j$ *in the Standard Model*, *J. Phys.* **G 42** (2015) 085002 [arXiv:1506.02718] [INSPIRE].

[32] I.P. Ivanov, *Building and testing models with extended Higgs sectors*, *Prog. Part. Nucl. Phys.* **95** (2017) 160 [arXiv:1702.03776] [INSPIRE].

[33] D. Atwood, L. Reina and A. Soni, *Phenomenology of two Higgs doublet models with flavor changing neutral currents*, *Phys. Rev.* **D 55** (1997) 3156 [hep-ph/9609279] [INSPIRE].

[34] F. Mahmoudi and O. Stal, *Flavor constraints on the two-Higgs-doublet model with general Yukawa couplings*, *Phys. Rev.* **D 81** (2010) 035016 [arXiv:0907.1791] [INSPIRE].

[35] A. Crivellin, A. Kokulu and C. Greub, *Flavor-phenomenology of two-Higgs-doublet models with generic Yukawa structure*, *Phys. Rev.* **D 87** (2013) 094031 [arXiv:1303.5877] [INSPIRE].

[36] A. Celis, V. Ilisie and A. Pich, *LHC constraints on two-Higgs doublet models*, *JHEP* **07** (2013) 053 [arXiv:1302.4022] [INSPIRE].

[37] B. Dumont, J.F. Gunion, Y. Jiang and S. Kraml, *Constraints on and future prospects for Two-Higgs-Doublet Models in light of the LHC Higgs signal*, *Phys. Rev.* **D 90** (2014) 035021 [arXiv:1405.3584] [INSPIRE].

[38] F.J. Botella, G.C. Branco, M. Nebot and M.N. Rebelo, *Flavour Changing Higgs Couplings in a Class of Two Higgs Doublet Models*, *Eur. Phys. J.* **C 76** (2016) 161 [arXiv:1508.05101] [INSPIRE].

[39] A. Arhrib, R. Benbrik, C.-H. Chen, M. Gomez-Bock and S. Semlali, *Two-Higgs-doublet type-II and -III models and* $t \to ch$ *at the LHC*, *Eur. Phys. J.* **C 76** (2016) 328 [arXiv:1508.06490] [INSPIRE].

JHEP02(2020)147

[40] F. del Aguila and M.J. Bowick, *The Possibility of New Fermions With $\Delta I = 0$ Mass*, *Nucl. Phys.* **B 224** (1983) 107 [INSPIRE].

[41] G.C. Branco and L. Lavoura, *On the Addition of Vector Like Quarks to the Standard Model*, *Nucl. Phys.* **B 278** (1986) 738 [INSPIRE].

[42] L. Lavoura and J.P. Silva, *Bounds on the mixing of the down type quarks with vector-like singlet quarks*, *Phys. Rev.* **D 47** (1993) 1117 [INSPIRE].

[43] F. del Aguila, J.A. Aguilar-Saavedra and R. Miquel, *Constraints on top couplings in models with exotic quarks*, *Phys. Rev. Lett.* **82** (1999) 1628 [hep-ph/9808400] [INSPIRE].

[44] F. del Aguila, M. Pérez-Victoria and J. Santiago, *Effective description of quark mixing*, *Phys. Lett.* **B 492** (2000) 98 [hep-ph/0007160] [INSPIRE].

[45] F. del Aguila, M. Pérez-Victoria and J. Santiago, *Observable contributions of new exotic quarks to quark mixing*, *JHEP* **09** (2000) 011 [hep-ph/0007316] [INSPIRE].

[46] G. Barenboim, F.J. Botella and O. Vives, *Constraining Models with Vector-Like Fermions from FCNC in K and B Physics*, *Nucl. Phys.* **B 613** (2001) 285 [hep-ph/0105306] [INSPIRE].

[47] F.J. Botella, G.C. Branco and M. Nebot, *The Hunt for New Physics in the Flavour Sector with up vector-like quarks*, *JHEP* **12** (2012) 040 [arXiv:1207.4440] [INSPIRE].

[48] S. Fajfer, A. Greljo, J.F. Kamenik and I. Mustac, *Light Higgs and Vector-like Quarks without Prejudice*, *JHEP* **07** (2013) 155 [arXiv:1304.4219] [INSPIRE].

[49] J.A. Aguilar-Saavedra, R. Benbrik, S. Heinemeyer and M. Pérez-Victoria, *Handbook of vectorlike quarks: Mixing and single production*, *Phys. Rev.* **D 88** (2013) 094010 [arXiv:1306.0572] [INSPIRE].

[50] S.A.R. Ellis, R.M. Godbole, S. Gopalakrishna and J.D. Wells, *Survey of vector-like fermion extensions of the Standard Model and their phenomenological implications*, *JHEP* **09** (2014) 130 [arXiv:1404.4398] [INSPIRE].

[51] K. Ishiwata, Z. Ligeti and M.B. Wise, *New Vector-Like Fermions and Flavor Physics*, *JHEP* **10** (2015) 027 [arXiv:1506.03484] [INSPIRE].

[52] C. Bobeth, A.J. Buras, A. Celis and M. Jung, *Patterns of Flavour Violation in Models with Vector-Like Quarks*, *JHEP* **04** (2017) 079 [arXiv:1609.04783] [INSPIRE].

[53] J.F. Gunion and H.E. Haber, *The CP conserving two Higgs doublet model: The Approach to the decoupling limit*, *Phys. Rev.* **D 67** (2003) 075019 [hep-ph/0207010] [INSPIRE].

[54] S. Davidson and H.E. Haber, *Basis-independent methods for the two-Higgs-doublet model*, *Phys. Rev.* **D 72** (2005) 035004 [*Erratum ibid.* **D 72** (2005) 099902] [hep-ph/0504050] [INSPIRE].

[55] A. Djouadi, *The Anatomy of electro-weak symmetry breaking. II. The Higgs bosons in the minimal supersymmetric model*, *Phys. Rept.* **459** (2008) 1 [hep-ph/0503173] [INSPIRE].

[56] G.C. Branco, P.M. Ferreira, L. Lavoura, M.N. Rebelo, M. Sher and J.P. Silva, *Theory and phenomenology of two-Higgs-doublet models*, *Phys. Rept.* **516** (2012) 1 [arXiv:1106.0034] [INSPIRE].

[57] H. Georgi and D.V. Nanopoulos, *Suppression of Flavor Changing Effects From Neutral Spinless Meson Exchange in Gauge Theories*, *Phys. Lett.* **B 82** (1979) 95 [INSPIRE].

[58] J.F. Donoghue and L.F. Li, *Properties of Charged Higgs Bosons*, *Phys. Rev.* **D 19** (1979) 945 [INSPIRE].

JHEP02(2020)147

[59] F.J. Botella and J.P. Silva, *Jarlskog-like invariants for theories with scalars and fermions*, *Phys. Rev.* **D 51** (1995) 3870 [hep-ph/9411288] [INSPIRE].

[60] H.E. Haber and D. O'Neil, *Basis-independent methods for the two-Higgs-doublet model. II. The Significance of* $\tan\beta$, *Phys. Rev.* **D 74** (2006) 015018 [*Erratum ibid.* **D 74** (2006) 059905] [hep-ph/0602242] [INSPIRE].

[61] D. Eriksson, J. Rathsman and O. Stal, *2HDMC: Two-Higgs-Doublet Model Calculator Physics and Manual*, *Comput. Phys. Commun.* **181** (2010) 189 [arXiv:0902.0851] [INSPIRE].

[62] I.P. Ivanov and J.P. Silva, *Tree-level metastability bounds for the most general two Higgs doublet model*, *Phys. Rev.* **D 92** (2015) 055017 [arXiv:1507.05100] [INSPIRE].

[63] H. Huffel and G. Pocsik, *Unitarity Bounds on Higgs Boson Masses in the Weinberg-Salam Model With Two Higgs Doublets*, *Z. Phys.* **C 8** (1981) 13 [INSPIRE].

[64] I.F. Ginzburg and I.P. Ivanov, *Tree-level unitarity constraints in the most general 2HDM*, *Phys. Rev.* **D 72** (2005) 115010 [hep-ph/0508020] [INSPIRE].

[65] S. Kanemura and K. Yagyu, *Unitarity bound in the most general two Higgs doublet model*, *Phys. Lett.* **B 751** (2015) 289 [arXiv:1509.06060] [INSPIRE].

[66] B. Grinstein, C.W. Murphy and P. Uttayarat, *One-loop corrections to the perturbative unitarity bounds in the CP-conserving two-Higgs doublet model with a softly broken* $\mathbb{Z}_2$ *symmetry*, *JHEP* **06** (2016) 070 [arXiv:1512.04567] [INSPIRE].

[67] G. Altarelli and R. Barbieri, *Vacuum polarization effects of new physics on electroweak processes*, *Phys. Lett.* **B 253** (1991) 161 [INSPIRE].

[68] M.E. Peskin and T. Takeuchi, *Estimation of oblique electroweak corrections*, *Phys. Rev.* **D 46** (1992) 381 [INSPIRE].

[69] W. Grimus, L. Lavoura, O.M. Ogreid and P. Osland, *The Oblique parameters in multi-Higgs-doublet models*, *Nucl. Phys.* **B 801** (2008) 81 [arXiv:0802.4353] [INSPIRE].

[70] H.E. Haber and D. O'Neil, *Basis-independent methods for the two-Higgs-doublet model III: The CP-conserving limit, custodial symmetry and the oblique parameters S, T, U*, *Phys. Rev.* **D 83** (2011) 055017 [arXiv:1011.6188] [INSPIRE].

[71] GFITTER Group, *The global electroweak fit at NNLO and prospects for the LHC and ILC*, *Eur. Phys. J.* **C 74** (2014) 3046 [arXiv:1407.3792] [INSPIRE].

[72] ATLAS and CMS collaborations, *Combined Measurement of the Higgs Boson Mass in pp Collisions at* $\sqrt{s} = 7$ *and* 8 *TeV with the ATLAS and CMS Experiments*, *Phys. Rev. Lett.* **114** (2015) 191803 [arXiv:1503.07589] [INSPIRE].

[73] CMS collaboration, *Search for Higgs boson off-shell production in proton-proton collisions at* 7 *and* 8 *TeV and derivation of constraints on its total decay width*, *JHEP* **09** (2016) 051 [arXiv:1605.02329] [INSPIRE].

[74] J.F. Gunion, H.E. Haber, G.L. Kane and S. Dawson, *The Higgs Hunter's Guide*, *Front. Phys.* **80** (2000) 1 [INSPIRE].

[75] ATLAS and CMS collaborations, *Measurements of the Higgs boson production and decay rates and constraints on its couplings from a combined ATLAS and CMS analysis of the LHC pp collision data at* $\sqrt{s} = 7$ *and* 8 *TeV*, *JHEP* **08** (2016) 045 [arXiv:1606.02266] [INSPIRE].

JHEP02(2020)147

[76] CMS collaboration, *Evidence for the Higgs boson decay to a bottom quark-antiquark pair*, *Phys. Lett.* **B 780** (2018) 501 [arXiv:1709.07497] [INSPIRE].

[77] ATLAS collaboration, *Evidence for the $H \to b\bar{b}$ decay with the ATLAS detector*, *JHEP* **12** (2017) 024 [arXiv:1708.03299] [INSPIRE].

[78] CMS collaboration, *Observation of the Higgs boson decay to a pair of τ leptons with the CMS detector*, *Phys. Lett.* **B 779** (2018) 283 [arXiv:1708.00373] [INSPIRE].

[79] HFLAV collaboration, *Averages of b-hadron, c-hadron and τ-lepton properties as of summer 2016*, *Eur. Phys. J.* **C 77** (2017) 895 [arXiv:1612.07233] [INSPIRE].

[80] G. Buchalla, A.J. Buras and M.E. Lautenbacher, *Weak decays beyond leading logarithms*, *Rev. Mod. Phys.* **68** (1996) 1125 [hep-ph/9512380v1] [INSPIRE].

[81] A. Celis, J. Fuentes-Martín, A. Vicente and J. Virto, *DsixTools: The Standard Model Effective Field Theory Toolkit*, *Eur. Phys. J.* **C 77** (2017) 405 [arXiv:1704.04504v3] [INSPIRE].

[82] J. Aebischer, M. Fael, C. Greub and J. Virto, *B physics Beyond the Standard Model at One Loop: Complete Renormalization Group Evolution below the Electroweak Scale*, *JHEP* **09** (2017) 158 [arXiv:1704.06639v1] [INSPIRE].

[83] D. Becirevic, V. Giménez, G. Martinelli, M. Papinutto and J. Reyes, *Combined relativistic and static analysis for all $\Delta B = 2$ operators*, *Nucl. Phys. Proc. Suppl.* **106** (2002) 385 [hep-lat/0110117] [INSPIRE].

[84] T. Inami and C.S. Lim, *Effects of superheavy quarks and leptons in low-energy weak processes $K_L \to \mu\bar{\mu}$, $K^+ \to \pi^+\nu\bar{\nu}$ and $K^0 \leftrightarrow \bar{K}^0$*, *Prog. Theor. Phys.* **65** (1981) 297 [*Erratum ibid.* **65** (1981) 1772] [UT-KOMABA-80-8] [INSPIRE].

[85] L. Di Luzio, M. Kirk and A. Lenz, *Updated B_s-mixing constraints on new physics models for $b \to s\ell^+\ell^-$ anomalies*, *Phys. Rev.* **D 97** (2018) 095035 [arXiv:1712.06572] [INSPIRE].

[86] A.J. Buras, M. Jamin and P.H. Weisz, *Leading and Next-to-leading QCD Corrections to ϵ Parameter and $B^0 - \bar{B}^0$ Mixing in the Presence of a Heavy Top Quark*, *Nucl. Phys.* **B 347** (1990) 491 [INSPIRE].

[87] A. Lenz and U. Nierste, *Theoretical update of $B_s - \bar{B}_s$ mixing*, *JHEP* **06** (2007) 072 [hep-ph/0612167] [INSPIRE].

[88] A. Di Iura, J. Herrero-Garcia and D. Meloni, *Phenomenology of* SU(5) *low-energy realizations: the diphoton excess and Higgs flavor violation*, *Nucl. Phys.* **B 911** (2016) 388 [arXiv:1606.08785] [INSPIRE].

[89] M. Misiak et al., *Estimate of $\mathcal{B}(\bar{B} \to X_s\gamma)$ at $O(\alpha_s^2)$*, *Phys. Rev. Lett.* **98** (2007) 022002 [hep-ph/0609232] [INSPIRE].

[90] M. Misiak et al., *Updated NNLO QCD predictions for the weak radiative B-meson decays*, *Phys. Rev. Lett.* **114** (2015) 221801 [arXiv:1503.01789] [INSPIRE].

[91] T. Hermann, M. Misiak and M. Steinhauser, *$\bar{B} \to X_s\gamma$ in the Two Higgs Doublet Model up to Next-to-Next-to-Leading Order in QCD*, *JHEP* **11** (2012) 036 [arXiv:1208.2788] [INSPIRE].

[92] M. Ciuchini, G. Degrassi, P. Gambino and G.F. Giudice, *Next-to-leading QCD corrections to $B \to X_s\gamma$: Standard model and two Higgs doublet model*, *Nucl. Phys.* **B 527** (1998) 21 [hep-ph/9710335] [INSPIRE].

JHEP02(2020)147

[93] F.M. Borzumati and C. Greub, *Two Higgs doublet model predictions for $\bar{B} \to X_s\gamma$ in NLO QCD*, *Phys. Rev.* **D 58** (1998) 074004 [hep-ph/9802391] [INSPIRE].

[94] M. Misiak and M. Steinhauser, *NNLO QCD corrections to the $\bar{B} \to X_s\gamma$ matrix elements using interpolation in m_c*, *Nucl. Phys.* **B 764** (2007) 62 [hep-ph/0609241] [INSPIRE].

[95] M. Benzke, S.J. Lee, M. Neubert and G. Paz, *Factorization at Subleading Power and Irreducible Uncertainties in $\bar{B} \to X_s\gamma$ Decay*, *JHEP* **08** (2010) 099 [arXiv:1003.5012] [INSPIRE].

[96] F. Feroz, M.P. Hobson and M. Bridges, *MultiNest: an efficient and robust Bayesian inference tool for cosmology and particle physics*, *Mon. Not. Roy. Astron. Soc.* **398** (2009) 1601 [arXiv:0809.3437] [INSPIRE].

[97] P. Scott, *Pippi — painless parsing, post-processing and plotting of posterior and likelihood samples*, *Eur. Phys. J. Plus* **127** (2012) 138 [arXiv:1206.2245] [INSPIRE].

[98] ATLAS collaboration, *Measurement of the production cross section for a Higgs boson in association with a vector boson in the $H \to WW^* \to \ell\nu\ell\nu$ channel in pp collisions at $\sqrt{s} = 13$ TeV with the ATLAS detector*, *Phys. Lett.* **B 798** (2019) 134949 [arXiv:1903.10052] [INSPIRE].

[99] ATLAS collaboration, *Measurements of gluon-gluon fusion and vector-boson fusion Higgs boson production cross-sections in the $H \to WW^* \to e\nu\mu\nu$ decay channel in pp collisions at $\sqrt{s} = 13$ TeV with the ATLAS detector*, *Phys. Lett.* **B 789** (2019) 508 [arXiv:1808.09054] [INSPIRE].

[100] ATLAS collaboration, *Evidence for the associated production of the Higgs boson and a top quark pair with the ATLAS detector*, *Phys. Rev.* **D 97** (2018) 072003 [arXiv:1712.08891] [INSPIRE].

[101] M.A. Arroyo-Ureña, R. Gaitán-Lozano, E.A. Herrera-Chacón, J.H. Montes de Oca Y. and T.A. Valencia-Pérez, *Search for the $t \to ch$ decay at hadron colliders*, *JHEP* **07** (2019) 041 [arXiv:1903.02718] [INSPIRE].

[102] A. Papaefstathiou and G. Tetlalmatzi-Xolocotzi, *Rare top quark decays at a 100 TeV proton-proton collider: $t \to bWZ$ and $t \to hc$*, *Eur. Phys. J.* **C 78** (2018) 214 [arXiv:1712.06332] [INSPIRE].

[103] UTFIT collaboration, *The Unitarity Triangle Fit in the Standard Model and Hadronic Parameters from Lattice QCD: A Reappraisal after the Measurements of Δm_s and $BR(B \to \tau\nu_\tau)$*, *JHEP* **10** (2006) 081 [hep-ph/0606167] [INSPIRE].

[104] FERMILAB LATTICE, MILC and TUMQCD collaborations, *Up-, down-, strange-, charm- and bottom-quark masses from four-flavor lattice QCD*, *Phys. Rev.* **D 98** (2018) 054517 [arXiv:1802.04248] [INSPIRE].

[105] F. Jegerlehner, M.Y. Kalmykov and B.A. Kniehl, *On the difference between the pole and the $\overline{MS}$ masses of the top quark at the electroweak scale*, *Phys. Lett.* **B 722** (2013) 123 [arXiv:1212.4319] [INSPIRE].

[106] V. Lubicz and C. Tarantino, *Flavour physics and Lattice QCD: Averages of lattice inputs for the Unitarity Triangle Analysis*, *Nuovo Cim.* **B 123** (2008) 674 [arXiv:0807.4605] [INSPIRE].

JHEP02(2020)147